Knee

7

Marcelo Bordalo-Rodrigues and Lawrence M. White

Learning Objectives

- To recognize normal anatomy of the knee.
- To recognize abnormalities of main knee structures.
- To diagnose knee abnormalities on MRI.

7.1 Introduction

Imaging has a crucial role in detecting internal derangements of the knee, and knowledge of pathologic conditions has increased. Imaging aspects of meniscal, ligament, tendinous, and chondral lesions will be discussed in this chapter.

7.2 Menisci

7.2.1 Anatomy and Function

Menisci are fibrocartilaginous structures that serve to enlarge the articular surfaces of the femoral condyles and tibia, as well as promote shock absorption and load distribution across the joint [1, 2]. The menisci are composed of an anterior horn, a body, and a posterior horn and do not have identical morphologies. The lateral meniscus has a circular shape and a looser capsular attachment. Posteriorly the lateral meniscus is separated from the capsule by the popliteus tendon and sheath (popliteus hiatus). The anterior and posterior horns of the lateral meniscus have the same size. The medial meniscus has a semicircular shape and is firmly attached to the capsule and less mobile than the lateral meniscus. For that reason, it is more susceptible to tears. Its anterior horn is smaller than the posterior horn. Both menisci have anterior and posterior insertions at the tibia (meniscal roots) [2].

The transverse meniscal ligament connects and stabilizes the anterior horns of the menisci and can mimic a tear on sagittal MR images [3] (Fig. 7.1).

Meniscofemoral ligaments connect the posterior horn of the lateral meniscus to the inner aspect of the medial femoral condyle, with the anterior meniscofemoral ligament of Humphrey and posterior meniscofemoral ligament of Wrisberg denoted based on their course, anterior and posterior to the posterior cruciate ligament, respectively [4].

Popliteomeniscal fascicles are fibrous structures that connect the posterior horn of the lateral meniscus to the joint capsule around the popliteal tendon sheath and help form the popliteal hiatus [1, 2]. They stabilize the posterior horn of the lateral meniscus during knee motion. Lesions of these fascicles are highly associated with tears of the posterior horn of the lateral meniscus [5].

An oblique meniscomeniscal ligament is an uncommon variant with a reported prevalence of 1–4% consisting of a ligamentous connection between the anterior horn of one meniscus and the posterior horn of the opposite meniscus and can mimic a displaced meniscal fragment [6].

7.2.2 Anatomic Variants

Discoid meniscus is an enlarged meniscus with central extension onto the tibial articular surface. It is 10–20 times more common in the lateral meniscus [7]. There are four distinct variants of discoid meniscus, according to the percentage of tibial plateau coverage: (1) complete (covers entire tibial plateau), (2) partial (covers 80% or less of the tibial plateau), (3) Wrisberg (thickened posterior horn, lacking posterior meniscal attachments), and (4) ring-shaped variant

M. Bordalo-Rodrigues (✉)
Department of Radiology, University of Sao Paulo Medical School, Sao Paulo, SP, Brazil

L. M. White
Department of Medical Imaging, University of Toronto, Toronto, ON, Canada
e-mail: Lawrence.white@uhn.ca

J. Hodler et al. (eds.), *Musculoskeletal Diseases 2021–2024*, IDKD Springer Series,
https://doi.org/10.1007/978-3-030-71281-5_7

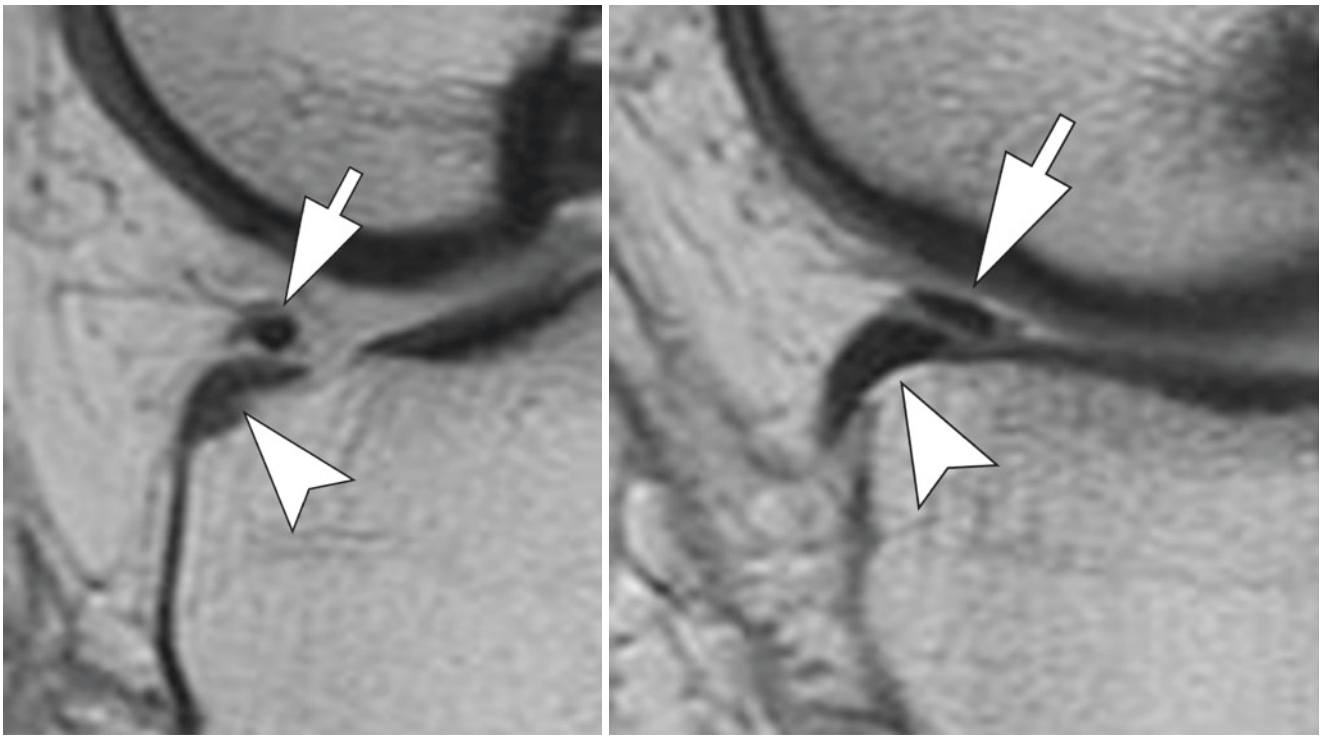

Fig. 7.1 Transverse meniscal ligament. Consecutive sagittal proton density (PD)-weighted images of the knee. The transverse meniscal ligament (arrows) inserting on the anterior horn of the medial meniscus (arrowheads), mimicking a tear

with connection between the anterior and posterior horns (can mimic a bucket-handle tear) [8, 9] (Fig. 7.2).

Meniscal flounce is a single symmetric fold along the free edge of the medial meniscus, secondary to flexion of the knee and physiologic redundancy of the free edge of the meniscus. It is not a tear; however, it may mimic a radial tear on coronal images [10, 11].

Meniscal ossicle is a rare developmental, degenerative, or post-traumatic variant, more common on the posterior horn of the medial meniscus. It may mimic an ossified loose body on radiographs and a tear on MRI.

7.2.3 Meniscal Tears

Meniscal tears are most common at the posterior horn of the medial meniscus; however, in young patients with acute injuries, lateral meniscal tears are common. There is an increased incidence of peripheral meniscal tears in cases of anterior cruciate ligament tears [12].

Normal menisci should have low signal on MR imaging. Linear or globular intrameniscal high signal is normally observed in children and at peripheral portions of the meniscus (red zone), due to high vascularization. MR accuracy for diagnosis of a meniscal tear is 90–95%, using arthroscopy as gold standard [12, 13]. MR imaging criteria for a meniscal tear are meniscal morphologic distortion (in absence of prior surgery) or intrameniscal high signal intensity extending to an articular surface, seen on two or more consecutive slices [13, 14]. If these criteria are seen in only one slice, the finding should be reported as a "possible tear" [15]. Increased intrameniscal high signal without articular surface extension should not be reported as tear and usually represents mucinous degeneration are acute intrasubstance contusion due to trauma [7].

Tears should be described accurately by radiologists in order to guide appropriate treatment. Most meniscal tear classification systems are based on the direction and location of the tear. **Longitudinal tears** run parallel to the long (circumferential) axis of the meniscus and perpendicular to tibial plateau. **Vertical longitudinal tears** are oriented in a superior-inferior direction and extend to one or both articular surfaces (Fig. 7.3). **Horizontal tears** also run parallel to the long axis of the meniscus but, however, are oriented parallel to the tibial plateau (Fig. 7.4). Typically, horizontal meniscal tears communicate with the free edge or articular surface of the meniscus. **Radial tears** are vertical meniscal tears which run perpendicular to the long axis of the meniscus and the tibial plateau. Typically, radial tears appear as linear signal changes perpendicular to the free/inner edge of the meniscus. Depending on the tear location and extent, unique MR signs may be present in the setting of a radial tear, including the "ghost meniscus" and the "truncated triangle" signs (Fig. 7.5). **A root tear** is typically a radial tear involving one

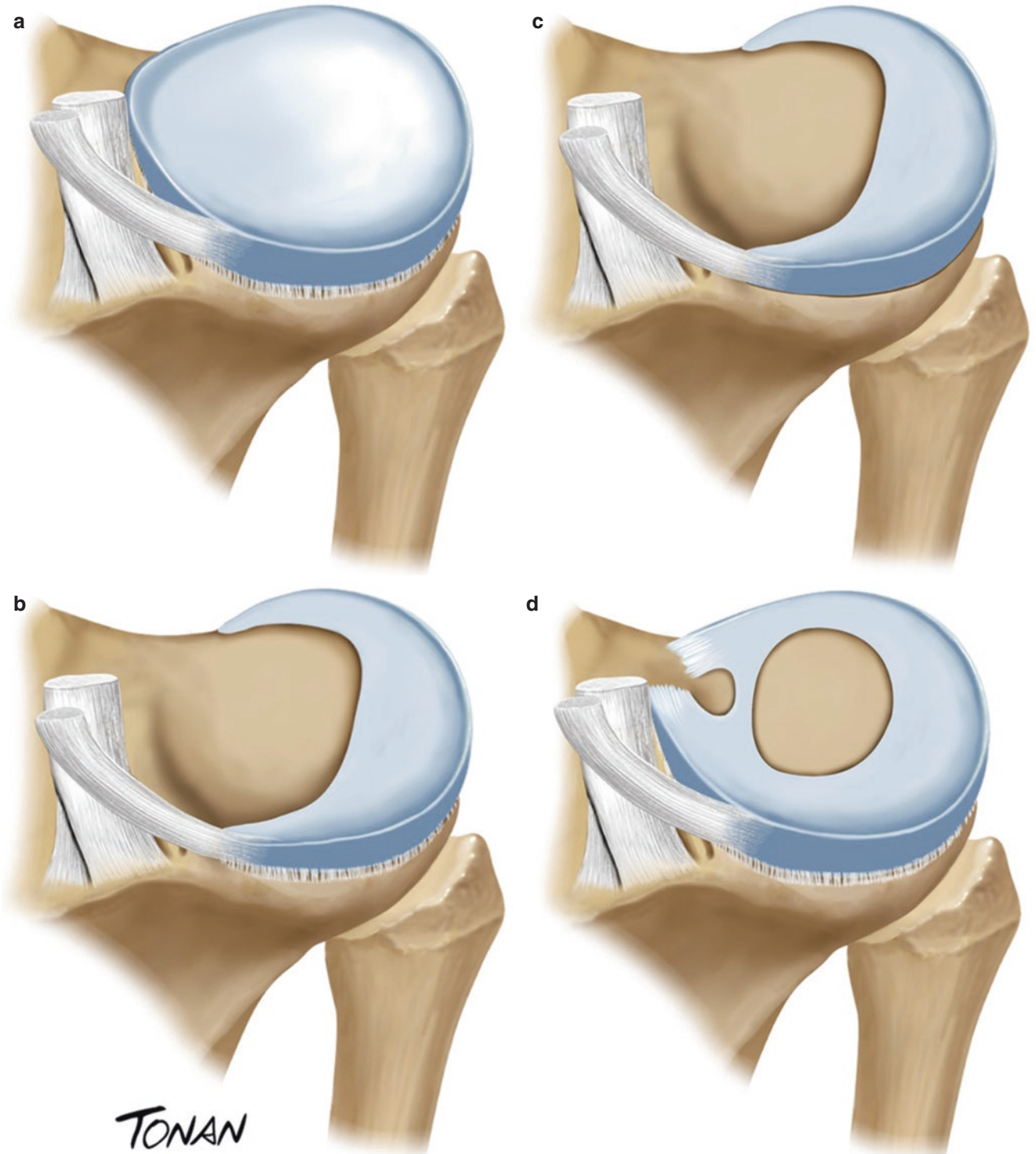

Fig. 7.2 Discoid meniscus variants. Schematic drawing demonstrates (**a**) complete discoid meniscus; (**b**) partial discoid meniscus; (**c**) Wrisberg variant (note absence of posterior meniscal attachments); and (**d**) ring-shaped discoid meniscus. (Reproduced with Permission by Rodrigo Tonan)

of the meniscal roots, most commonly the posterior root of the medial meniscus. Complete root tears are associated with meniscal extrusion and progressive femorotibial degenerative changes (Fig. 7.6). **Complex tears** are a combination of longitudinal, horizontal, and radial tear components (at least two) [7]. Meniscal tears which communicate with the periphery of the meniscus may be associated with the formation of a parameniscal cyst.

A **meniscal "ramp lesion"** is a longitudinal vertical meniscal tear at the peripheral attachment of the posterior horn of the medial meniscus [16]. It is strongly associated with ACL tears and reflective of traumatic injury of the meniscocapsular junction [17, 18]. MR findings of a ramp lesion are meniscocapsular separation (with or without intervening fluid-like signal), peripheral meniscal irregularities, and far peripheral longitudinal tearing of the medial meniscus [19] (Fig. 7.7).

A **zip lesion** or Wrisberg rip is a longitudinal vertical meniscal tear progressing from the distal insertion of the posterior meniscofemoral ligament (Wrisberg) through the posterior horn of the lateral meniscus, which may be seen in association with ACL tears [20–22] (Fig. 7.8).

Displaced meniscal tears include free fragments or flap lesions associated with a meniscal tear. Small meniscal displaced fragments may not be seen at arthroscopy; thus,

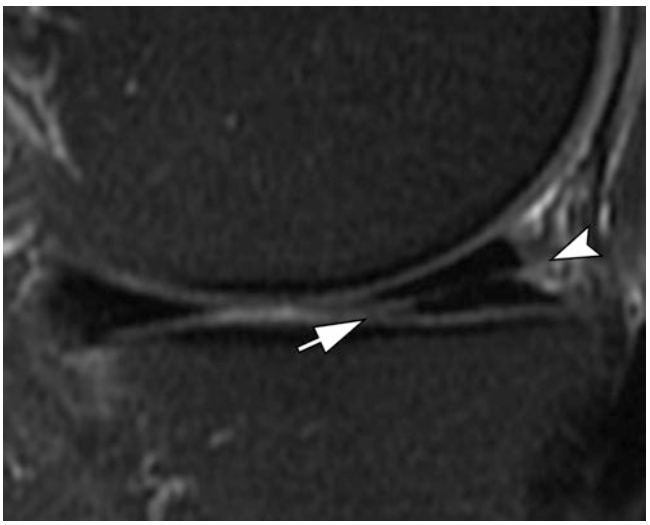

Fig. 7.3 Horizontal tear. Sagittal T2-weighted image of the knee with fat suppression. There is a horizontal tear of the mesial meniscus, extending to the free edge (arrow) and posterior capsular surface (arrowhead)

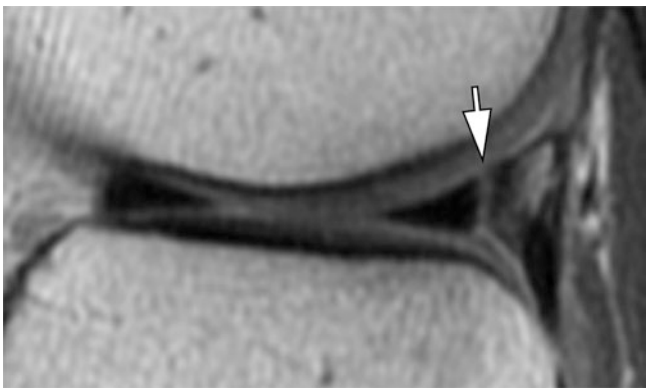

Fig. 7.4 Vertical tear. Sagittal PD-weighted image of the knee. A peripheral vertical tear extending to superior and inferior articular surfaces (arrow)

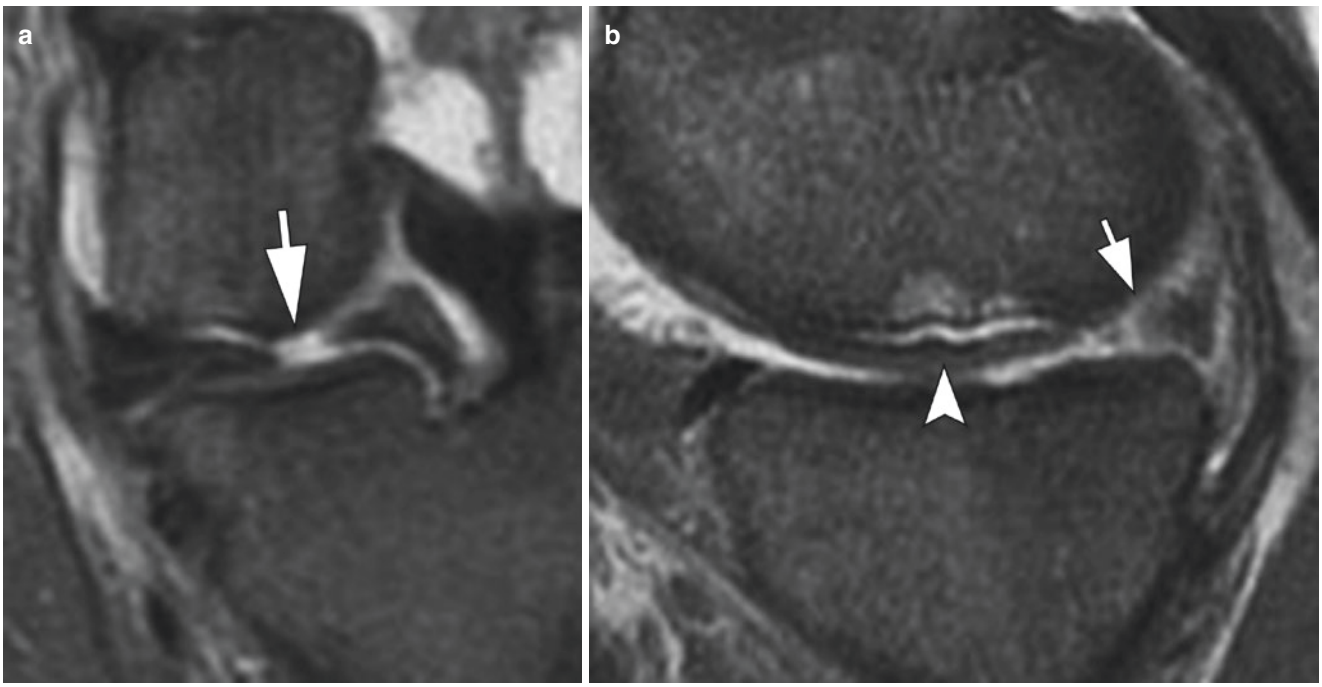

Fig. 7.5 Radial tear. (**a**) Coronal and (**b**) sagittal T2-weighted images of the knee with fat suppression. Linear tear of the posterior horn of the medial meniscus, perpendicular to free edge (white arrow). On the sagittal plane, the radial tear has a "truncated triangle" aspect (black arrow). There is also a subchondral fracture of the medial femoral condyle (arrowhead)

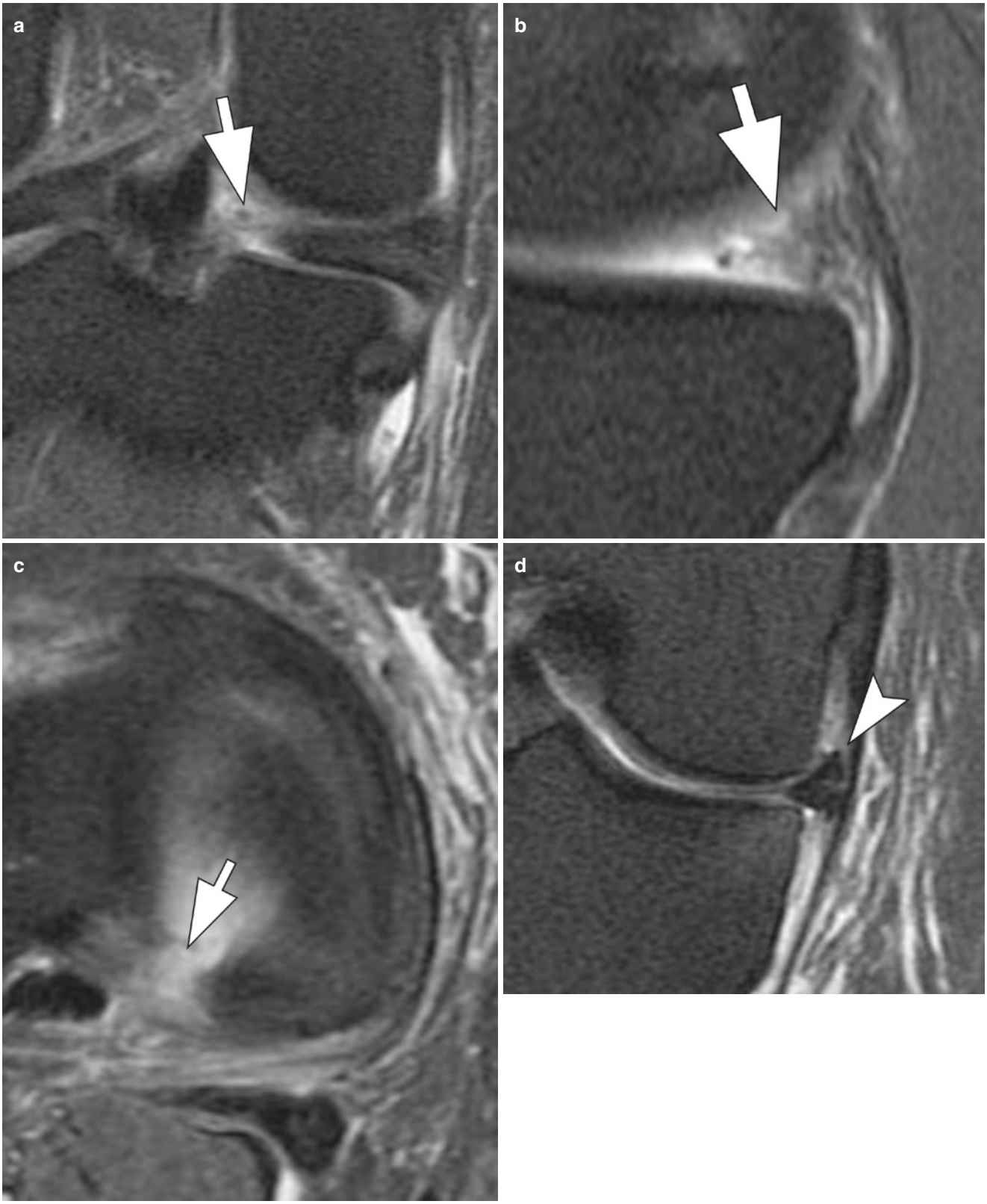

Fig. 7.6 Root tear. (**a**) Coronal; (**b**) sagittal; (**c**) axial; and (**d**) coronal T2-weighted images of the knee with fat suppression. There is a complete radial tear in the posterior root of the medial meniscus (arrows), with a "ghost meniscus" sign on the sagittal image (arrow in **b**). There is an associated extrusion of the body (arrowhead)

Fig. 7.7 Ramp lesion. Sagittal T2-weighted image of the knee with fat suppression. Vertical tear of the posterior meniscocapsular junction extending to the peripheral aspect of the medial meniscus (arrow)

identification on MR images can be of critical importance in patient management and preoperative planning. Fragments are more common arising from the medial meniscus and may be displaced around the PCL, in the intercondylar notch, or peripherally along the superior/inferior recesses of the joint. In absence of prior surgery, a diminutive morphology of the meniscus should alert the radiologist to search for a displaced meniscal flap (Fig. 7.9). A bucket handle tear is a displaced vertical longitudinal tear associated with central displacement of the inner part of the meniscus. Bucket handle tears are more common in the medial meniscus, and several imaging signs have been described associated with bucket handle meniscal tears at MR imaging including a double PCL sign, absent bow tie, double anterior horn, fragment in the notch, and small posterior horn [23, 24] (Fig. 7.10).

Key Point

- Signal abnormalities that extend to meniscal surface and displaced meniscal fragments are important features to be identified on MRI.

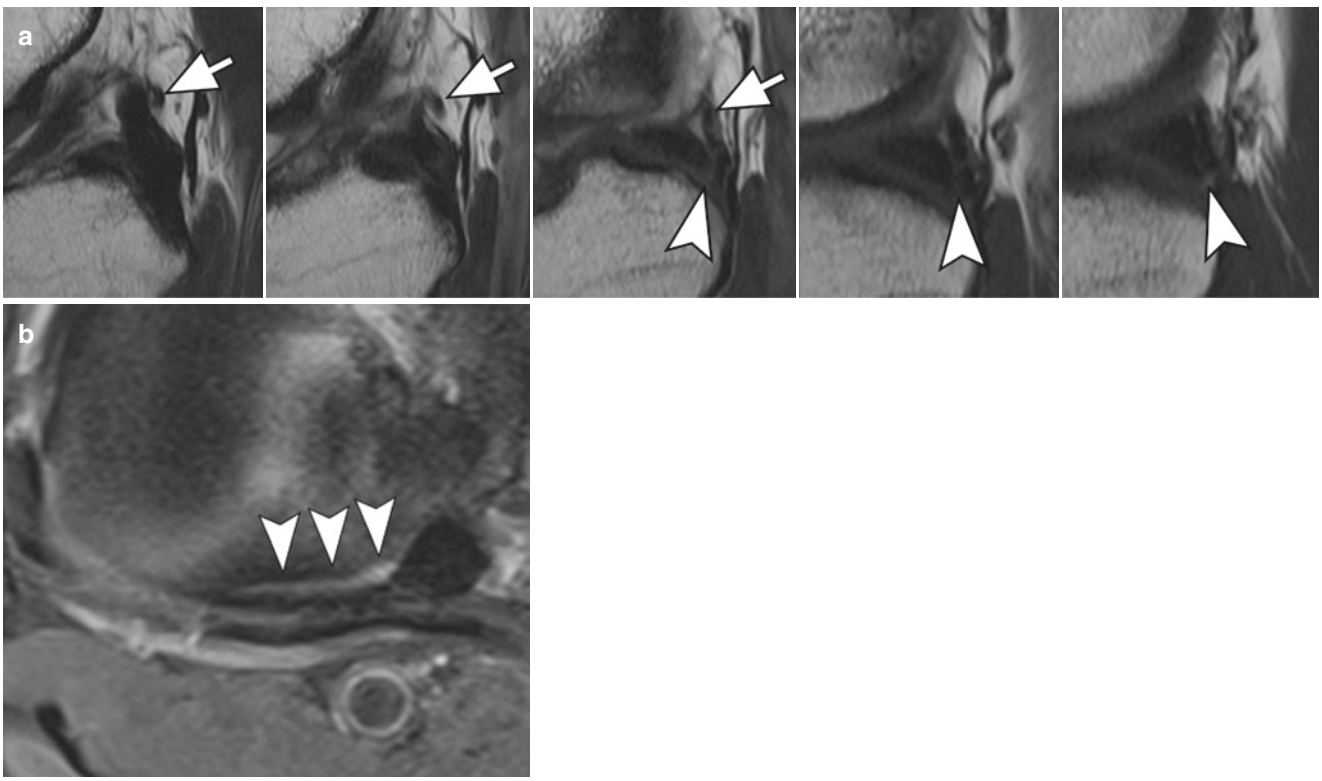

Fig. 7.8 Zip lesion. (**a**) Consecutive sagittal PD-weighted images and (**b**) axial T2-weighted image show the Wrisberg ligament inserting in the posterior horn of the lateral meniscus (arrows) and a peripheral vertical longitudinal tear of this meniscus (arrowheads)

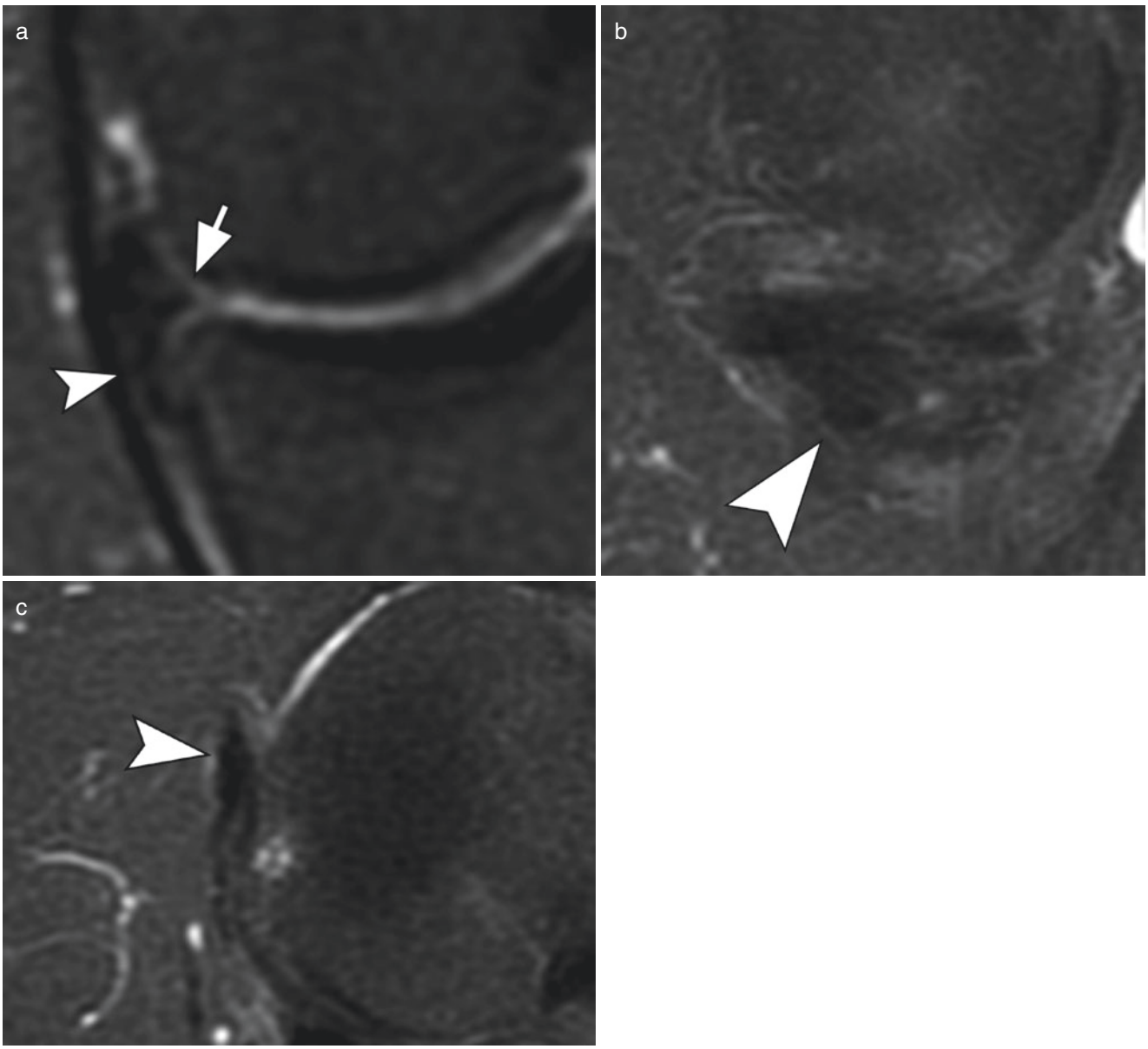

Fig. 7.9 Displaced meniscal tear. (**a**) Coronal; (**b**) sagittal; and (**c**) axial T2-weighted images of the knee with fat suppression. There is a complex tear at the body of medial meniscus with increase in size (arrow). A displaced inferior meniscal flap is associated with this tear (arrowheads)

7.3 Ligaments

7.3.1 Cruciate Ligaments

7.3.1.1 Anterior Cruciate Ligament

Anatomy and Function

The anterior cruciate ligament (ACL) is an intracapsular and extrasynovial structure that is proximally attached to the medial surface of the lateral femoral condyle and a distal attachment on the tibia, anterolateral to the tibial spines. The distal insertion of the ACL is stronger and broader than its proximal femoral attachment. The fascicles are anatomically divided into two bundles, the posterolateral and anteromedial bands. The anteromedial bundle is the main restraint to anterior translation of the tibia during knee flexion, and the posterolateral bundle is the predominant restraint to anterior tibial translation during knee extension and also serves as a restraint against internal rotation of the tibia. The bundles can be visualized as distinct bands along the middle to distal thirds of the ligament, especially on axial and coronal MR images. Increased intrasubstance linear signal intensity parallel to the long axis of the ligament may be seen within the

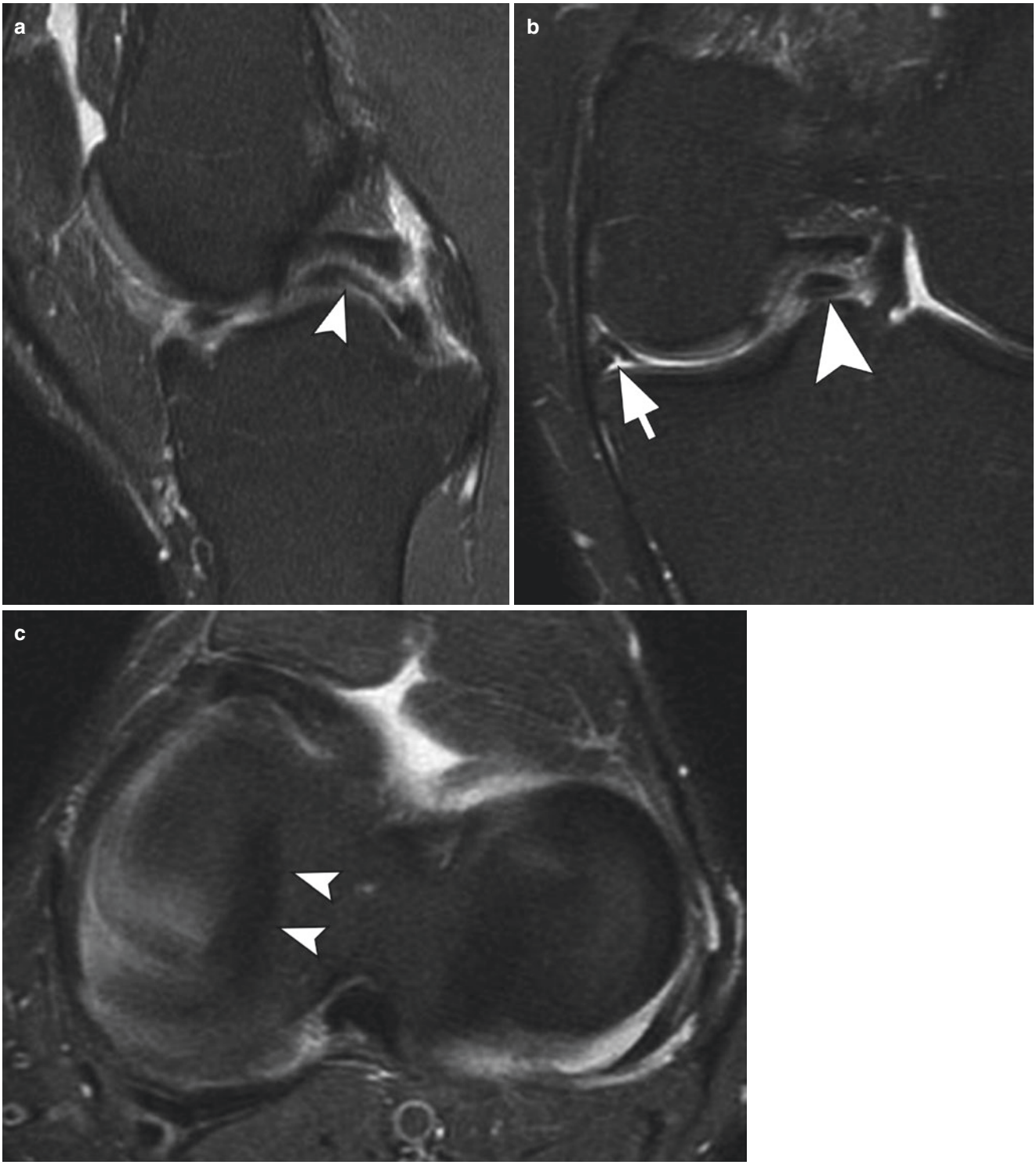

Fig. 7.10 Bucket handle tear. (**a**) Sagittal; (**b**) coronal; and (**c**) axial T2-weighted images of the knee with fat suppression. A complete longitudinal tear of the medial meniscus (arrow) with a displaced meniscal fragment to the intercondylar notch (arrowheads), with a double PCL sign (arrowhead in **b**)

distal ACL, presumably related to areas of fat and synovium between ligament fibers [2, 25]. Normal orientation of the ACL in the sagittal plane is parallel or within 9° to the roof of the intercondylar notch.

ACL Tears

Anterior cruciate ligament tears are the most common ligamentous injuries in the knee, alone or in combination with other injuries. The classic mechanism of injury involved in

Fig. 7.11 ACL tear – direct sign. Sagittal T2-weighted image of the knee with fat suppression. Complete acute tear of the ACL with increased signal at the expected location of the ligament

ACL injury is indirect trauma with pivoting stress. MR imaging examination includes evaluation of axial, coronal, and sagittal images and is highly sensitive and specific in the diagnosis of ACL tears, with an accuracy of 90–95% [26, 27].

Direct MR signs of an ACL tear are focal ligamentous discontinuity, diffuse or focal signal intensity abnormality, and mass-like appearance in the expected location of the ACL [28] (Fig. 7.11). Increased signal within the ligament may be also seen in the setting of mucoid degeneration of the ACL, with characteristic features of an intact continuous ligament fibers with internal striated intervening T2 fluid-like signal (Fig. 7.12). Abnormal orientation of the ACL including a horizontally oriented distal ACL (angle of less than 45° between the distal ACL and the tibia) or a vertically oriented proximal ACL (angle greater than 15° between the proximal ligament and the roof of the intercondylar notch) is an additional finding which may be seen following ACL injury [29]. Distal fibers of the ACL may flip anteriorly following ACL disruption [30].

Indirect MR findings of an ACL tear have additionally been described. Such indirect findings of ACL injury include subchondral bone marrow edema at the central aspect of the lateral femoral condyle (sulcus terminalis) and posterior aspect of the lateral tibial plateau, secondary to pivot shift translational osseous impaction injuries (Fig. 7.13). Osseous injury is commonly associated with meniscal injury in the same compartment [31]. Anterior translation of 5 mm or more of the posterior aspect of the lateral tibial plateau in relation to the posterior aspect of the lateral femoral condyle is another indirect finding seen in the setting of ACL disruption [32]. Other signs described in the setting of an ACL tear include uncovering of the posterior horn of the lateral meniscus and "buckling" of the PCL [28]. In chronic ACL tears, the ligament may scar, and MR may not depict true severity/extent of the prior ACL injury. Scarring of the ACL can occur to the PCL, to the roof of the intercondylar notch, to its anatomical femoral origin, or as end-to-end scarring across torn tendon margins [33].

Partial tears account for 30% of all ACL injuries [30]. Such partial ACL injuries include isolated complete tearing of either the anteromedial (more common) or posterolateral bundles of the ligament or most commonly partial injuries of both bundles [34, 35]. MRI illustrates lower accuracy rates in the detection of partial ACL tears, ranging from 25 to 53% [35]. MR signs of partial ACL tearing include attenuation of the ACL, increased intraligamentous T2 signal with partial disruption of ligamentous fibers, and posterior ACL bowing on sagittal acquisitions [34–36] (Fig. 7.14).

7.3.1.2 Posterior Cruciate Ligament

Anatomy and Function

The posterior cruciate ligament (PCL), similar to the ACL, is also an intracapsular and extrasynovial ligament. The proximal origin of the PCL is along the lateral surface of the medial femoral condyle and its distal insertion in the midline of the proximal tibia, posteroinferior to tibial articular surface. The PCL is the major restraint to tibial posterior translation and anatomically consists of anterolateral and posteromedial fiber bundles. On MR imaging, the PCL has a homogeneous low signal intensity on all pulse sequences, with a curved "comma-shaped" morphologic appearance well depicted on sagittal imaging.

PCL Tears

Posterior cruciate ligament tears are less frequent than ACL tears due to its strong fibrous structure. The most common mechanism of PCL injury is a force applied to the anterior aspect of the proximal tibia with the knee flexed, driving the tibia posteriorly. Motor vehicle accidents in which the flexed knee hits the dashboard or in a fall upon the knee with knee flexion and posterior tibial translation are typical injuries leading to PCL disruption. Multiligamentous injuries are more common than isolated PCL tears. MR signs of PCL tears include complete focal ligamentous discontinuity and

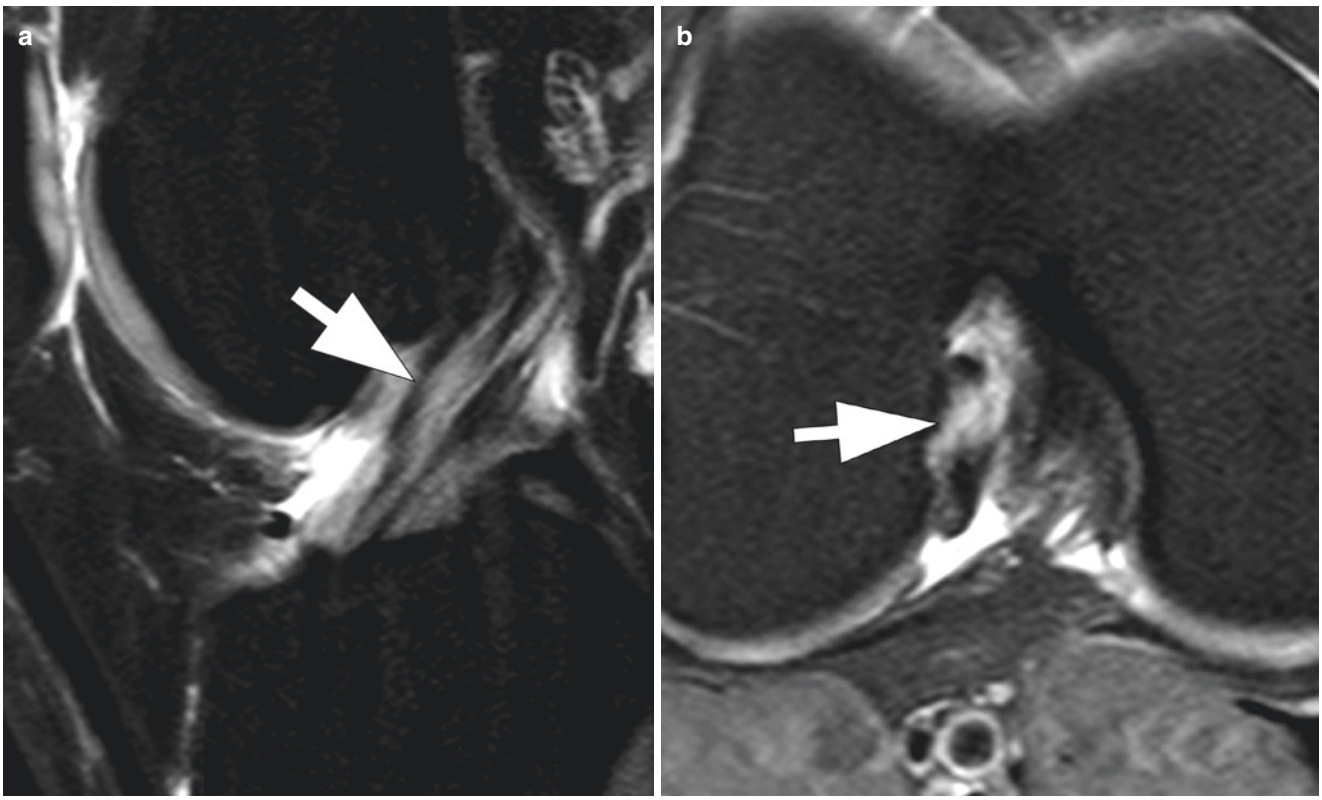

Fig. 7.12 ACL mucoid degeneration. (**a**) Sagittal and (**b**) axial T2-weighted images of the knee with fat suppression. There is increased signal within the ACL, with internal ligament striation preserved (arrows)

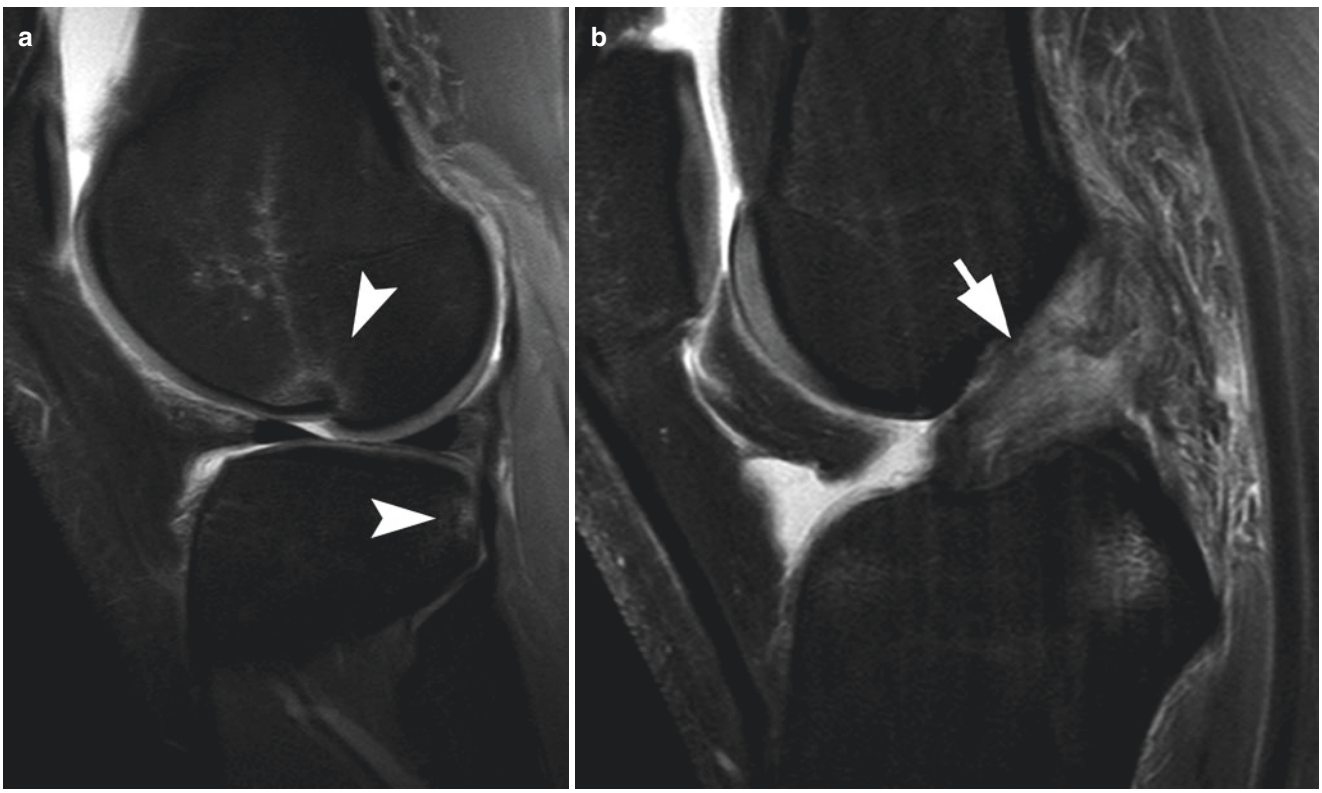

Fig. 7.13 ACL tear – indirect sign. (**a**) Sagittal T2-weighted image with fat suppression shows bone edema and impaction fractures at the central aspect of the lateral femoral condyle and posterior aspect of the lateral tibial plateau (arrowheads). (**b**) Sagittal T2-weighted image with fat suppression demonstrates the ACL tear (arrow)

Fig. 7.14 Partial ACL tear. Sagittal T2-weighted image of the knee with fat suppression shows increased thickening within the ACL with attenuation of ligamentous fibers (arrow)

Fig. 7.15 PCL tear. Sagittal PD-weighted image demonstrates PCL discontinuity with increased signal intensity (arrow)

increased T2 signal intensity of the PCL [37] (Fig. 7.15). Differentiation between complete and partial PCL tears is more difficult on MRI [38]. Mucoid degeneration of PCL can be suggested with a "tram-track" appearance, in which there is a peripheral rim of normal low signal intensity fibers [39] (Fig. 7.16). The PCL has a greater propensity to heal, when compared to ACL [40, 41]. Up to 28% of PCL tears can have a near normal MR appearance 6 months post injury [42]. Patients with combined PCL and posterolateral corner injuries and those with greater than 12 mm of posterior subluxation of the tibia on stress radiographs are less likely to demonstrate healing of PCL on follow-up MRI [40].

7.3.2 Medial Collateral Ligament

Anatomy and Function

The medial collateral ligament (MCL) serves as a primary stabilizer against valgus stress of the knee. It is composed of a superficial and a deep layer. The superficial layer or tibial collateral ligament is the strongest portion of MCL and most easily seen on MRI [43–45]. The deep layer is part of the joint capsule and composed of meniscofemoral and meniscotibial ligament extensions. An MCL bursa is situated between the superficial and deep portions of the MCL [46]. The superficial and deep components of the MCL are fused posteriorly by the posterior oblique ligament [44]. The superficial MCL has a femoral origin located posterior to the medial epicondyle and anterior to the adductor tubercle and a tibial attachment located approximately 5 cm distal to the joint line and deep to the pes anserinus tendons [43, 47, 48]. Some authors describe a second tibial attachment of the superficial MCL along the anterior arm of the semimembranosus [49].

MCL Tears

Medial collateral ligament tears are most commonly located along the proximal MCL and can be classified in three types [50]:

- Grade I: microscopic injury; MR demonstrates periligamentous edema, with normal hypointense signal of the MCL (Fig. 7.17).

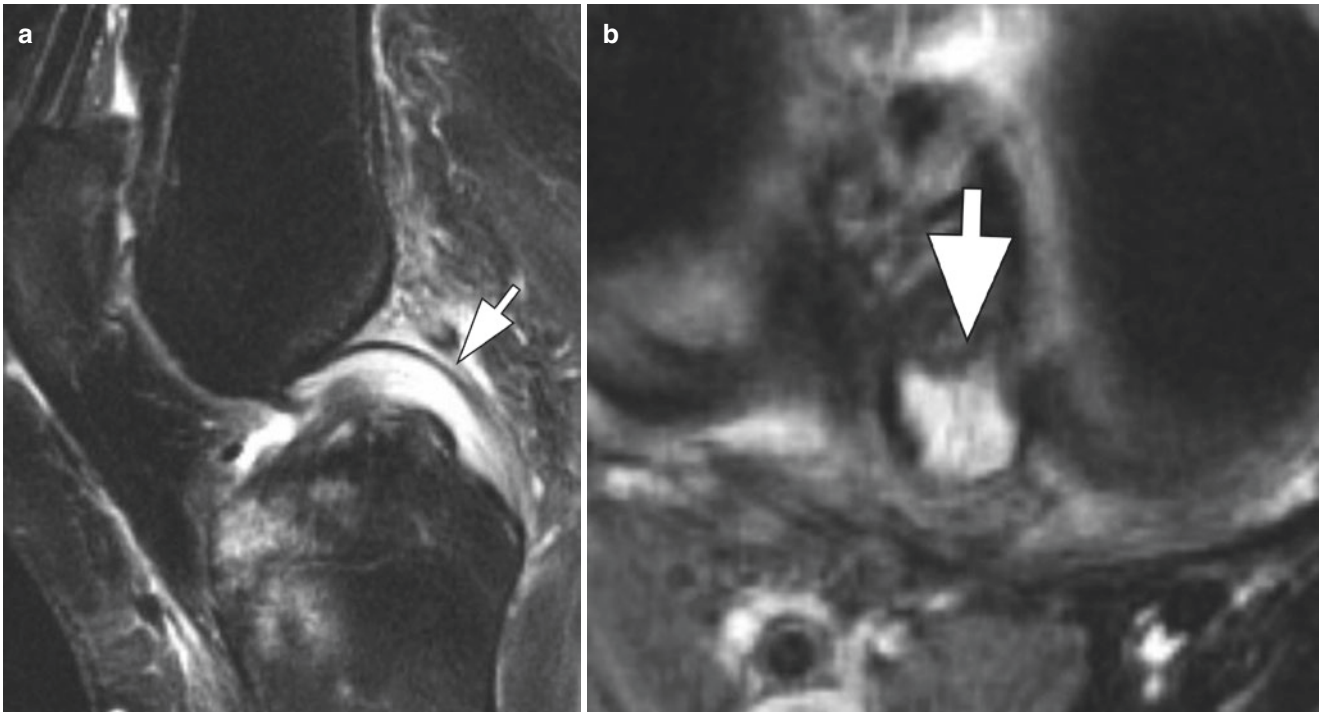

Fig. 7.16 PCL mucoid degeneration. (**a**) Sagittal and (**b**) axial T2-weighted images. There is increased signal within the PCL and a peripheral rim of intact fibers – "tram-trak" appearance (arrows)

Fig. 7.17 Grade I MCL tear. Coronal T2-weighted image with fat suppression. Edema surrounding the MCL (arrow)

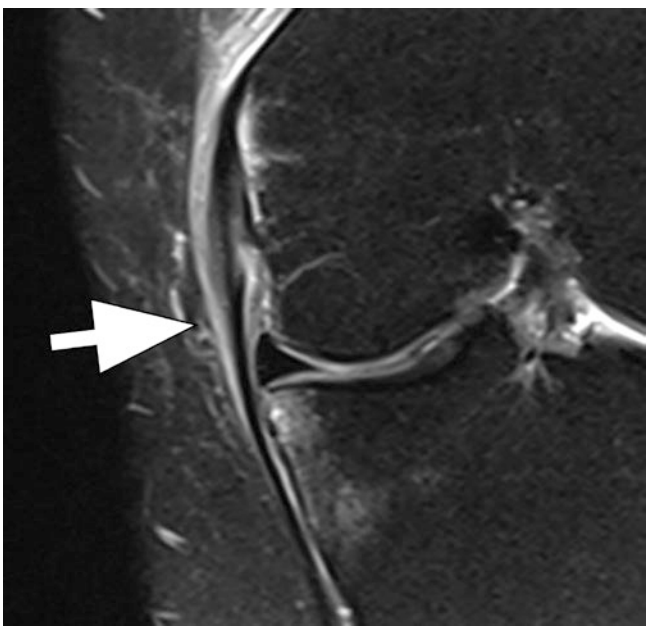

Fig. 7.18 Grade II MCL tear. Coronal T2-weighted image with fat suppression. Increased signal and thickening of the MCL (arrow)

– Grade II: partial tear; MR shows a thickened and edematous MCL with areas of increased intrasubstance signal, incomplete ligamentous disruption (Fig. 7.18).
– Grade III: complete tear; MR demonstrates complete discontinuity of superficial MCL.

Fig. 7.19 Grade III MCL tear. Coronal T2-weighted image with fat suppression. Complete distal MCL tear with proximal retraction and a "wavy" appearance (arrow)

Distal insertional tears of the superficial MCL are less common; however normal healing of far distal tears of the superficial MCL can be impaired due to poor blood supply and possible displacement of torn distal MCL ligament fibers. A "Stener-like" lesion of the distal superficial MCL occurs when there is ligament displacement superficial to the pes anserinus tendons [51]. A wavy morphologic appearance of the MCL without MCL disruption proximally is an imaging feature suggestive of a high-grade distal tear of the superficial MCL [52] (Fig. 7.19).

7.3.3 Posterolateral Corner

Anatomy and Function

The posterolateral corner structures are primary restraints of varus rotation and external tibial rotation and secondary restraints of anterior and posterior tibial translation.

The main stabilizers of the posterolateral corner complex are, from superficial to deep, include the lateral collateral ligament (or fibular collateral ligament), biceps femoris tendon, fabellofibular ligament, arcuate ligament, popliteofibular ligament, and popliteus tendon [53] (Fig. 7.20).

Lateral Collateral Ligament (Fibular Collateral Ligament)

The LCL is injured in about 23% of cases of posterolateral corner injury [54]. The lateral collateral ligament (LCL) or fibular collateral ligament is the primary stabilizer against

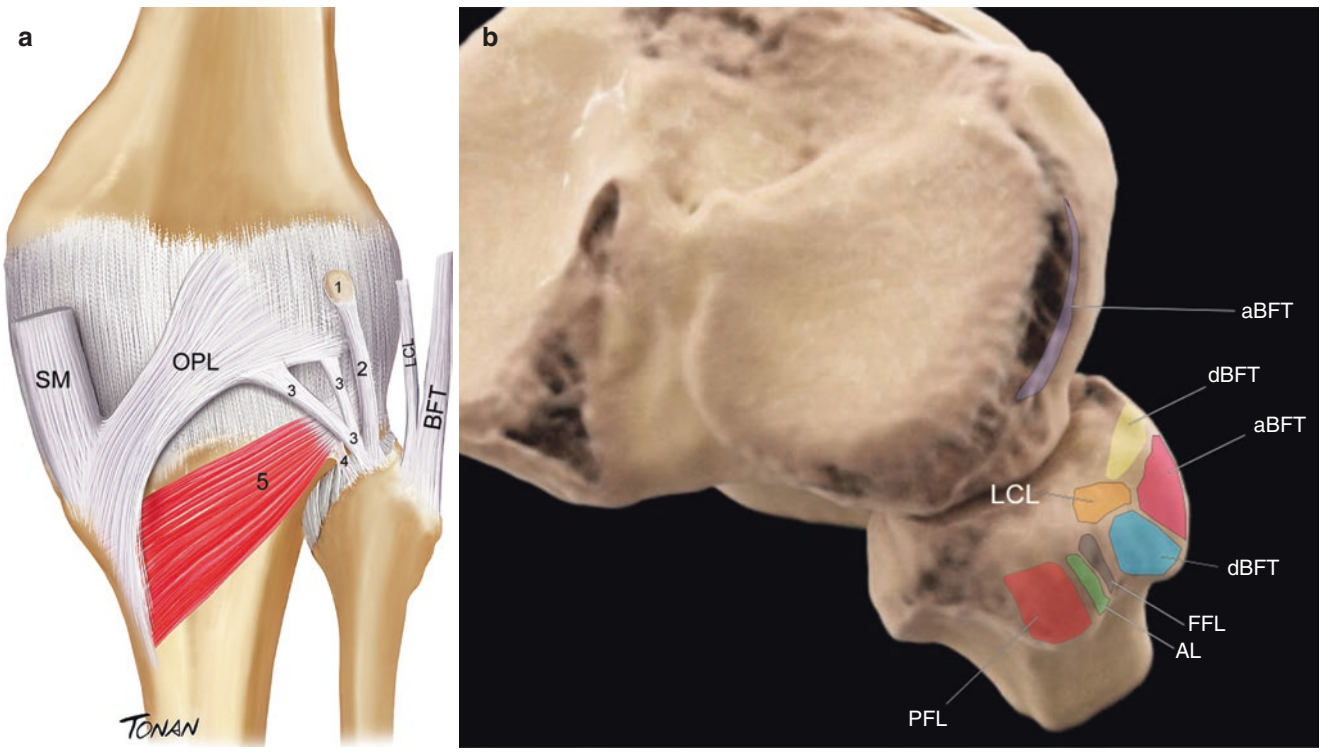

Fig. 7.20 Posterolateral corner anatomy. (**a**) Schematic drawing illustrating the posterolateral corner anatomy. *BFT* biceps femoris tendon, *LCL* lateral collateral ligament; (*1*), fabella; (*2*), fabellofibular ligament; (*3*), arcuate ligament; (*4*), popliteofibular ligament; and (*5*), popliteus muscle. Structures from the posteromedial corner are also demonstrated OPL, oblique popliteal ligament, and SM, semimembranosus tendon. (**b**) CT 3D reconstruction with posterolateral corner attachments. *aBFT* anterior arm of the biceps femoris tendon, *dBFT* direct arm of the biceps femoris tendon, *LCL* lateral collateral ligament, *FFL* fabellofibular ligament, *AL* arcuate ligament, *PFL* popliteofibular ligament. (Reproduced with Permission by Rodrigo Tonan)

Fig. 7.21 Lateral collateral ligament tear. Coronal T2-weighted image with fat suppression. Complete LCL tear (arrow)

varus stress of the knee and has a secondary role as a restraint to external rotation. It arises from the lateral femoral condyle and extends distally attaching to the lateral aspect of the fibular head, sometimes merging with the distal biceps femoris tendon to form a conjoined insertional tendon structure [55]. The lateral collateral ligament-biceps femoris bursa can be seen between these two structures [56].

Lateral collateral ligament tears can be classified as grades I (periligamentous edema), II (thickened and edematous LCL), and III (complete LCL disruption) (Fig. 7.21). Avulsion fracture of the fibular head by the LCL can be seen in the setting of an arcuate fracture [56, 57].

Biceps Femoris Tendon

The biceps femoris tendon descends posterior to the iliotibial tract and has two distal attachments identified on MRI: a direct arm (inserting on the posterolateral aspect of the fibular head) and an anterior arm (inserting to the anterior aspect of the fibular head and to the lateral tibial metaphysis) [55, 58, 59]. The biceps femoris tendon merges with the distal LCL and forms a conjoined insertional tendon. Injuries to the biceps femoris tendon include partial tears and tendinous and osseous avulsions from the fibular head.

Fabellofibular Ligament

The fabellofibular ligament is variably present but commonly seen when there is a bony fabella. The ligament runs from the fabella to the styloid process of the fibular head. When the fabella is absent, the ligament originates proximally to the posterior aspect of the supracondylar process of the femur [60]. The fabellofibular ligament may not be identified on MRI but when present is seen on coronal and sagittal planes posterior to genicular vessels and on axial plane anterior to the lateral head of the gastrocnemius tendon. Injuries include avulsions from the fibular head and partial−/complete-thickness tears.

Arcuate Ligament

The arcuate ligament is a thickening of the posterior joint capsule and has a Y shape. The medial limb attaches proximally to the oblique popliteal ligament, and the lateral limb attaches to the lateral femoral condyle. Distally, the medial and lateral limbs merge, attaching to the fibular styloid process, posterior to the insertion of the popliteofibular ligament. Identification of the arcuate ligament is variable on MRI, and when visualized the ligament is best depicted on axial and sagittal MR imaging acquisitions. Injury of the arcuate ligament is often implicated based on secondary MR imaging signs, especially edema and fluid/hemorrhage indicative of soft tissue injury immediately posterior to the popliteus tendon/hiatus [61] (Fig. 7.22). The presence of the arcuate sign (edema or avulsion fracture of the fibular head with intact LCL and biceps femoris tendon) is indicative of concurrent arcuate and popliteofibular ligament injuries [62].

Popliteofibular Ligament

The popliteofibular ligament is a major stabilizer of the posterolateral complex, originating at the popliteus tendon close to its myotendinous junction and inserting at the posterior aspect of the fibular styloid process [63]. MR visualization of this ligament is difficult, with improved visualization described with dedicated oblique coronal or isotropic volumetric sequences [64]. Injuries are common in a setting of posterolateral instability [65], although direct identification of popliteofibular ligament disruption can be challenging at MRI (Fig. 7.23).

Popliteus Tendon

The popliteus tendon and muscle provide primary resistance to external rotation and secondary resistance to posterior tibial translation at the knee. The popliteus tendon is located deep to arcuate and fabellofibular ligaments, enters the joint, and attaches to the popliteus sulcus of the lateral femoral condyle, deep and anterior to the femoral origin of the LCL. Popliteomeniscal fascicles connect the popliteus

Fig. 7.22 Arcuate ligament strain. Coronal T2-weighted image with fat suppression. Increased signal and thickening of the arcuate ligament at its fibular attachment (arrow)

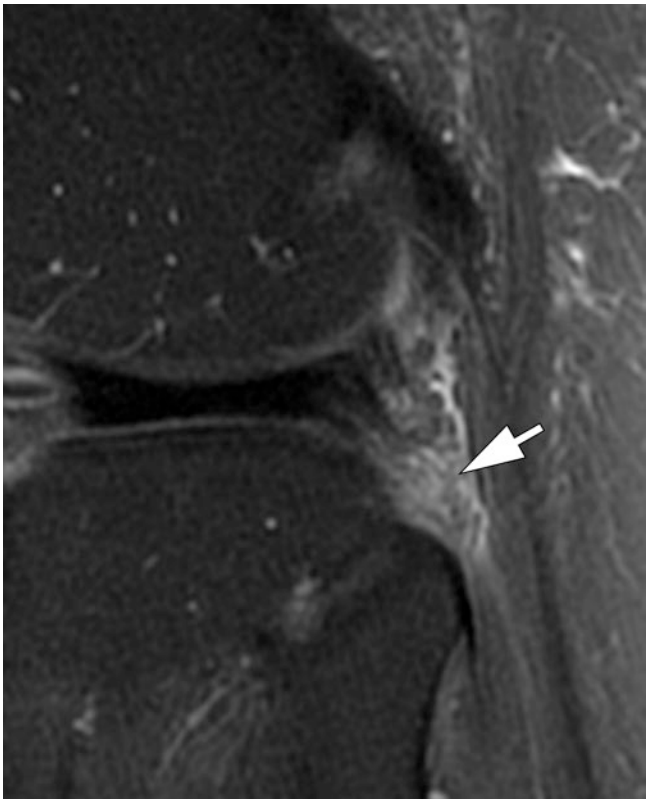

Fig. 7.23 Popliteofibular ligament strain. Sagittal T2-weighted image with fat suppression. Increased signal and thickening of the arcuate ligament at its fibular attachment (arrow)

tendon to the lateral meniscus, forming the popliteus hiatus. Popliteus injuries are more common at its myotendinous junction, although avulsions of the popliteus tendon at its femoral origin can occur (Fig. 7.24).

7.3.4 Posteromedial Corner

Anatomy and Function

The posteromedial corner structures are primary restraints to anteromedial rotatory instability and are composed of the posterior oblique ligament (POL), the oblique popliteal ligament (OPL), the semimembranosus tendon, and the meniscotibial ligament.

Posterior Oblique Ligament (POL)

The POL originates at the adductor tubercle, just posterior to the origin of the MCL, and extends distally composed of three arms: (1) central (or tibial) arm, attaching to the posteromedial aspect of the medial meniscus; (2) superior (or capsular) arm, attaching to the oblique popliteal ligament and capsule; and (3) distal arm, attaching to the semimembranosus tendon and tibia.

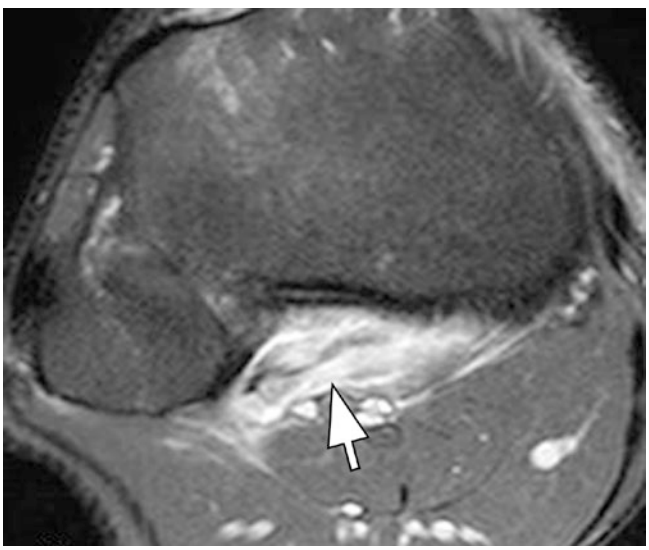

Fig. 7.24 Popliteus myotendinous strain. Axial T2-weighted image with fat suppression. Increased signal involving the popliteus myotendinous junction and muscle (arrow)

Oblique Popliteal Ligament (OPL)

The OPL is a broad ligamentous band that originates from the lateral aspect of the semimembranosus tendon and courses in a superolateral oblique direction across the

Fig. 7.25 Posterior oblique ligament tear. Coronal T2-weighted image with fat suppression. Complete tear of the POL (arrow) with exuberant surrounding edema

posterior aspect of the joint, forming part of the popliteal fossa and inserts at the fabella and posterolateral joint capsule (Fig. 7.20).

Semimembranosus Tendon

The distal semimembranosus tendon has five insertional arms: (1) direct arm (inserts at the posterior aspect of the medial tibial condyle), (2) capsular arm (merges with the capsular portion of the OPL), (3) anterior arm (courses anteriorly, deep to the POL, and inserts at the medial aspect of the tibia, deep to the MCL, (4) inferior arm (courses deep to MCL and POL and inserts proximal to tibial attachment of MCL, and (5) OPL extension. The semimembranosus is the main stabilizer of the posteromedial corner.

Injuries

Patients with anteromedial rotatory instability show injury of the POL in 99%, semimembranosus in 70%, and medial meniscus detachment in 30% of cases [66] (Figs. 7.25 and 7.26). There is an association between posteromedial corner injuries and ACL tears, although association between posteromedial and posterolateral corner injuries is uncommon. Adequate interpretation of these injuries is important, because posteromedial corner injury with anteromedial rotatory instability often requires surgical intervention.

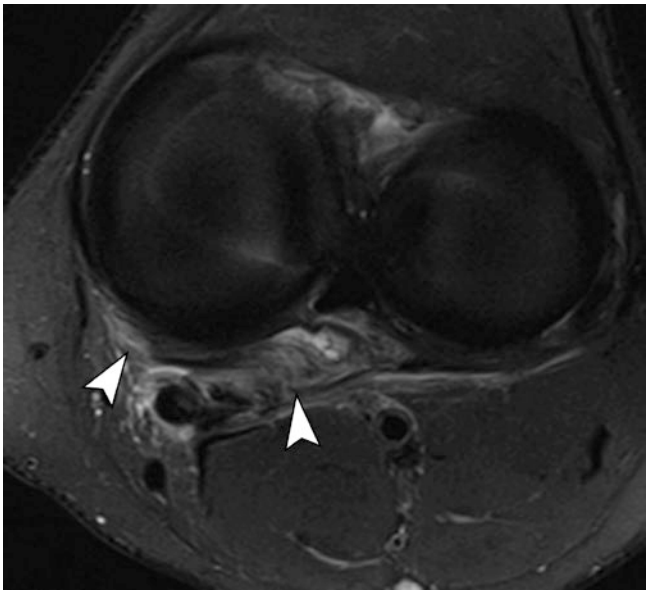

Fig. 7.26 Oblique popliteal ligament tear. Axial T2-weighted image with fat suppression. Increased signal and thickening of the OPL (arrow heads)

7.3.5 Anterolateral Ligament

Anatomy and Function

The anterolateral ligament (ALL) originates posterior and proximal to the lateral femoral epicondyle and courses anteroinferiorly overlapping the LCL toward the anterolateral tibia. As it approaches the joint line, some fibers attach to the lateral meniscus and anterolateral capsule [67, 68]. The tibial insertion is just behind Gerdy's tubercle (Fig. 7.27). ALL is an important stabilizer of internal rotation of the tibia. The ALL is identified in 90–100% of MR examinations [69, 70].

Injuries

A Segond fracture represents a bony injury of the tibial ALL insertion [71, 72]. ALL injuries are generally associated with ACL lesions (Fig. 7.28). Identification of ALL injuries is difficult, and secondary signs such as bony avulsion and edema at the anterolateral tibia may be useful findings in support of possible ALL injury.

7.3.6 Iliotibial Tract

Anatomy and Function

The iliotibial tract is composed of contributions from the tensor fascia lata and gluteus maximus muscles and from fibers of the fascia lata [73]. The superficial layer of the iliotibial tract inserts onto the Gerdy tubercle at the anterolateral tibia. The deep layer attaches the superficial

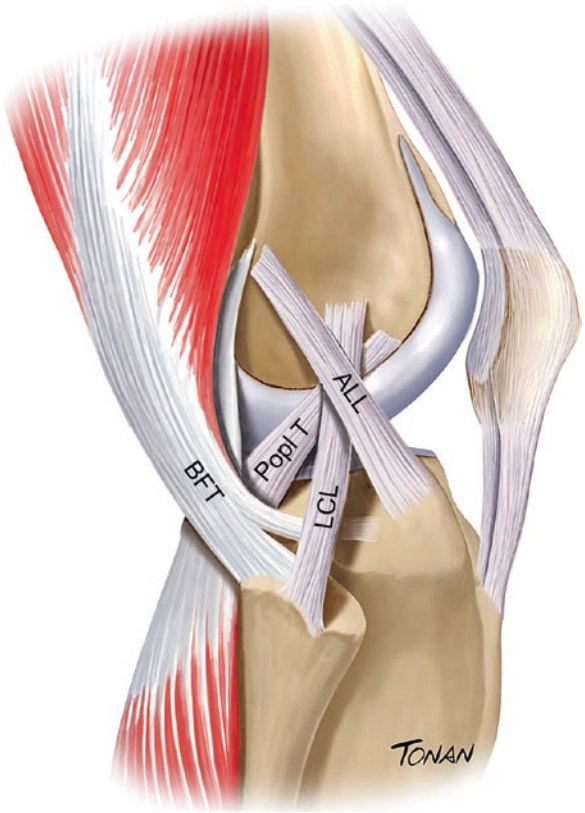

Fig. 7.27 Anterolateral ligament anatomy. Schematic drawing illustrating the anterolateral ligament anatomy and related structures. ALL, anterolateral ligament; LCL, lateral collateral ligament; Popl T, popliteus tendon; BFT, biceps femoris tendon. (Reproduced with Permission by Rodrigo Tonan)

layer to the supracondylar tubercle of the lateral femur with additional fibers inserting on lateral patellar retinaculum. The iliotibial tract provides anterolateral stability to the knee.

Iliotibial Band Syndrome

In general, iliotibial band syndrome or ilitotibial band friction syndrome is due to chronic overuse in activities such as cycling and running, with patients presenting with pain around the anterolateral femur due to repetitive friction between the iliotibial band and the underlying lateral femoral epicondyle. On MR, increased T2 soft tissue signal or a bursal fluid collection can be identified between the iliotibial tract and the lateral femoral condyle [73] (Fig. 7.29).

Injuries

In general, iliotibial tract tears occur in the setting of an acute knee trauma with other knee injuries, especially ACL tears and patellar dislocation. MRI demonstrates strains (edema superficial and deep to iliotibial tract) and partial (thickening and increased signal) and complete tears [74].

Key Point

- Adequate comprehension of detailed ligament anatomy is crucial to identify injuries on MRI.

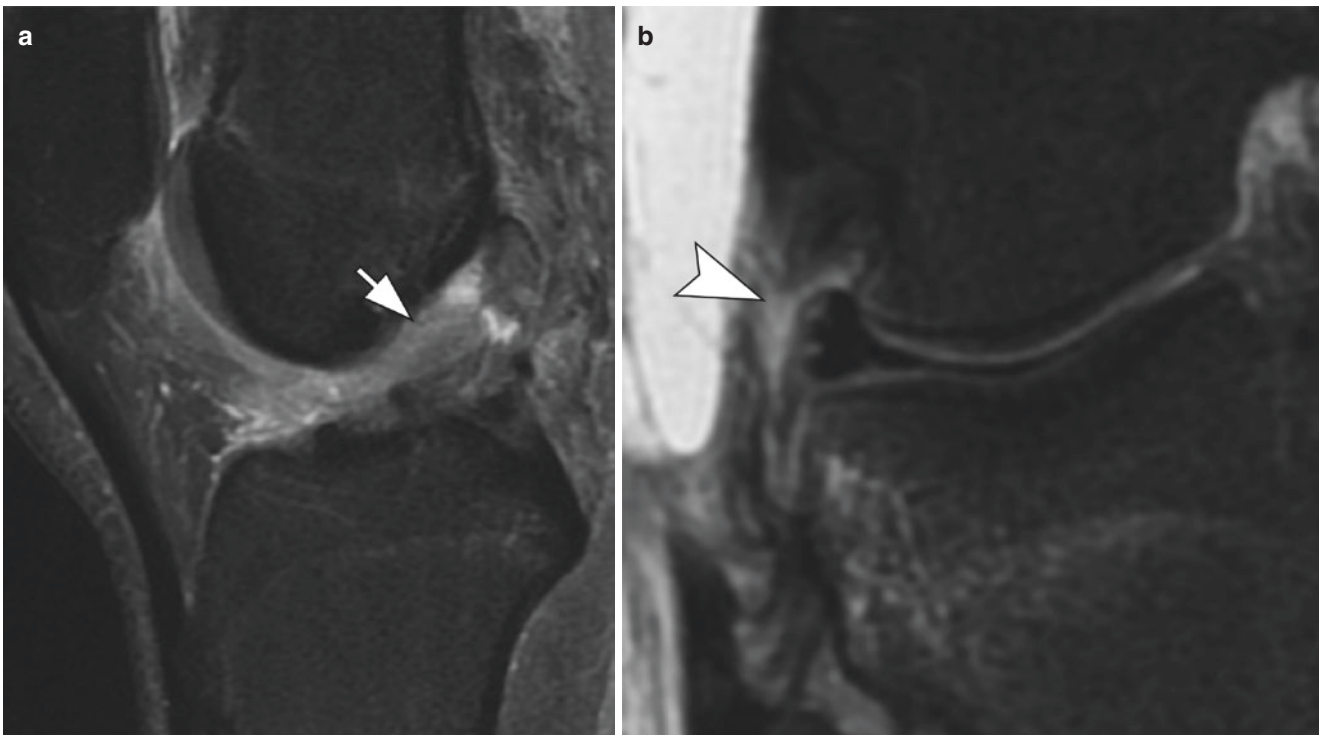

Fig. 7.28 Associated anterolateral and ACL tears. (**a**) Sagittal T2-weighted image with fat suppression showing an ACL tear (arrow). (**b**) Coronal T2-weighted image with fat suppression demonstrates a complete tear of the ALL (arrowhead)

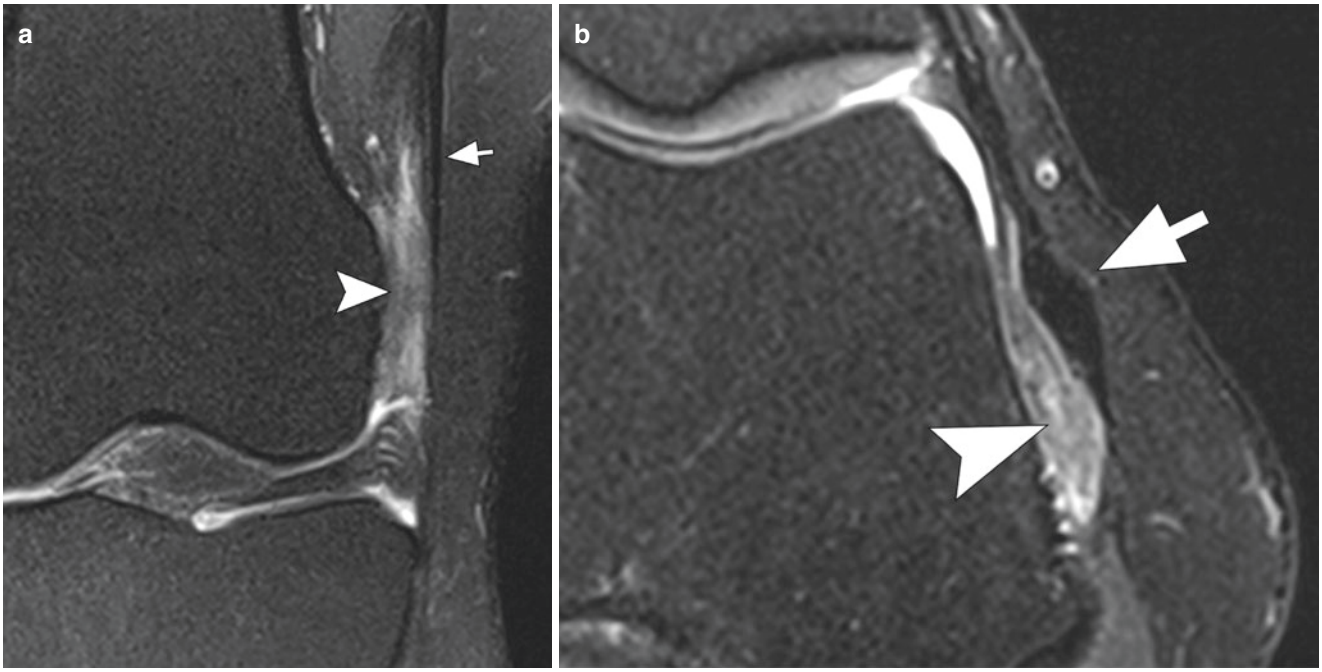

Fig. 7.29 Iliotibial band friction syndrome. (**a**) Coronal and (**b**) axial T2-weighted images with fat suppression demonstrate edema in the fat pad (arrowheads) between the lateral femoral condyle and the iliotibial band (arrows)

7.4 Tendons

7.4.1 Extensor Mechanism

Anatomy and Function

The extensor mechanism of the knee is composed of the quadriceps muscle group and tendon, the patella, the patellar retinaculum, and the patellar tendon. The tendons of the rectus femoris and vastus muscles converge distally to form the quadriceps tendon, inserting onto the superior pole of the patella. The quadriceps tendon has a tri-laminar appearance on MR imaging, with the rectus tendon forming the most superficial layer, the vastus medialis and lateralis forming the middle layer, and the vastus intermedius forming the deepest layer. Fat tissue interposes between the three tendon layers. The distal vastus medialis muscle has a longitudinal and an oblique portion, called the vastus medialis obliquus. Fascial extensions of the vastus medialis and lateralis form the patellar retinacula. Patellofemoral ligaments are focal thickening of the retinacula, similar to glenohumeral ligaments in the shoulder. The patellar tendon is composed by fibers of the rectus femoris and extends from the inferior pole of the patella to anterior tibial tuberosity.

Lateral Patellar Dislocation

Dynamic and anatomical conditions, including trochlear dysplasia and patella alta, can predispose to lateral patellar dislocation. In general, patellar dislocation is diagnosed on imaging retrospectively due to indirect findings on MRI: disruption of the medial retinaculum and medial patellofemoral ligament, typical bone marrow edema on the medial aspect of the patella and the anterolateral aspect of the lateral femoral condyle, osteochondral injuries (especially at the medial facet of the patella), and joint effusion/hemarthrosis [75] (Fig. 7.30).

Key Point

- Typical imaging features of lateral patellar dislocation are bone marrow edema at the medial aspect of the patella and anterolateral aspect of lateral femoral condyle, injury at the medial patellofemoral ligament, and joint effusion/hemarthrosis.

7.5 Cartilage

Hyaline cartilage is a fine connective tissue composed of a complex mesh of collagenous fibers, water, and proteoglycans. Chondral lesions include acute traumatic chondral or osteochondral injuries or chronic degenerative lesions which generally progress slowly with late clinical manifestations of disease.

MR imaging can provide information on chondral thickness, surface abnormalities, intrasubstance changes, and

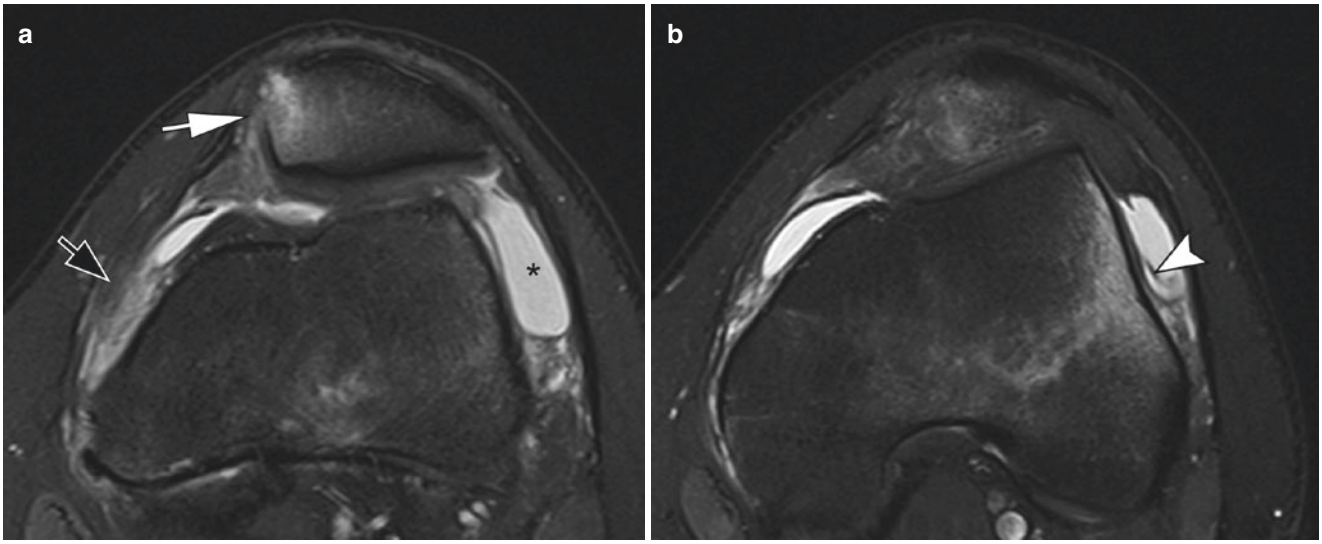

Fig. 7.30 Lateral patellar dislocation. Axial T2-weighted images of the knee with fat suppression. (**a**) Bone impaction with marrow edema at the medial facet of the patella (white arrow) and strain of the proximal aspect of the medial patellofemoral ligament (black arrow). * joint effusion. (**b**) Bone impaction with marrow edema at the anterolateral aspect of the lateral femoral condyle (arrowhead)

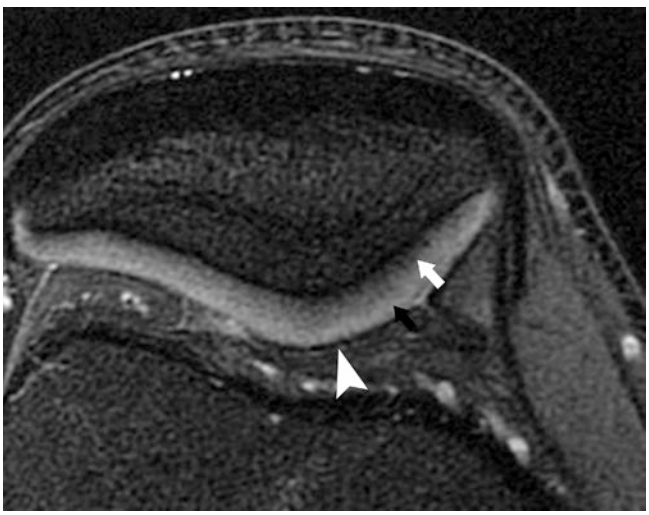

Fig. 7.31 Three-layer pattern of normal cartilage. Axial PD-weighted image with fat suppression. The deep layer shows low signal intensity (white arrow); the intermediate layer has high signal (black arrow), and the superficial layer has low signal (arrowhead)

subchondral bone abnormalities. Through more recent techniques, MRI can provide information on the biochemical and physiological characteristics of hyaline cartilage.

By using MRI with high spatial resolution and good soft tissue contrast, a three-layer pattern can be observed in the hyaline cartilage: 1) surface layer with low-intensity signal; 2) intermediate layer with high-intensity signal; and 3) deep layer with low-intensity signal and a "palisade" transition into the intermediate zone (Fig. 7.31). This three-layer appearance is more evident in thicker chondral surfaces, such as the patellar and femoral trochlear cartilage.

7.5.1 Chondral Lesions

The accuracy of MRI for detecting chondral lesions can be variable depending on MRI hardware and technique used, patient factors, as well as the etiology, extent/depth, and location of the lesion itself. The accuracy of MRI in diagnosis of degenerative chondral lesions is greater in deeper lesions, particularly in those that present more than 50% loss of chondral substance, with accuracy results in the literature ranging from 73 to 96% [76].

Chondral lesions are characterized on MRI by thickness and morphological abnormalities of hyaline cartilage as well as intrasubstance increased signal on proton density, T2-weighted and gradient echo sequences. One prior study demonstrated that 70% of chondral lesions presented as areas of high signal in relation to normal cartilage on proton density acquisitions, while 20% of lesions illustrated signal similar to that of normal cartilage (lesions not identified on MRI) and 10% illustrating low signal [77].

Chondral tapering, loss of definition, and chondral surface irregularities are additional features of chondral lesions that can be characterized on MR imaging. It has been demonstrated that the most frequent locations for chondral lesions are the medial femoral condyle (on its most internal aspect) and the lateral tibial plateau (on its most posterior portion) [78].

To classify chondral lesions using MRI, a system based on arthroscopic classifications is used [79]. Grade I lesions are shown as abnormalities of intrasubstance cartilage signal, corresponding to softening of the cartilage seen on arthroscopy. Grade II lesions are shown as morphologic irregularities and abnormalities of the surface

Fig. 7.32 Chondral injury classification. (A, B, and C) Axial and (D) sagittal PD-weighted images with fat suppression. (**a**) Increased signal of the superficial layer of the hyaline cartilage of the lateral facet of the patella with irregularities (arrow), indicating grade I lesion. There is also a deep chondral erosion (>50% – grade III) in the medial facet (arrowhead). (**b**) Fissure involving less than 50% of the hyaline cartilage of the lateral facet of the patella (arrow) (grade II lesion). (**c**) Chondral fissure involving more than 50% of the hyaline cartilage of the medial facet of the patella (arrow) (grade III lesion). (**d**) Deep chondral erosion in the lateral femoral condyle (arrow), reaching the subchondral bone associated with adjacent bone marrow edema (arrowheads) (grade IV lesion)

signal, indicating fibrillation or erosion of less than 50% of the chondral thickness. In Grade III lesions, there is loss of more than 50% of the chondral substance, and there may be small areas in which the bone surface is reached. Grade IV lesions indicate extensive full-thickness chondral defects with subchondral bone marrow edema [79, 80] (Fig. 7.32).

Loss of cartilage integrity may lead to abnormalities in the underlying subchondral bone, such as cysts, sclerosis, and osteophytosis, which can be detected on MRI. Another frequently associated finding is subchondral bone marrow edema-like signal changes, which studies suggest may predate and progress to subchondral cysts over time [81].

Chronic chondral lesions with detachment of cartilaginous fragments into the joint lead to chronic irritation of the synovium and may cause synovitis. In some cases, the synovial response can be very extensive and may take on a pseudotumoral appearance on imaging examinations (Fig. 7.33). Intraarticular loose bodies can be identified, especially in the suprapatellar recess, intercondylar notch, posterior to the femorotibial joint space and along the popliteal hiatus of the articulation (Fig. 7.34).

Key Point

- MRI underestimates size of chondral lesions. A complete description including cartilage, subchondral bone, and synovial abnormalities should be performed in a setting of chondral imaging.

Fig. 7.33 Pseudotumoral appearance of knee osteoarthrosis. Coronal T2-weighted image with fat suppression demonstrates complete and diffuse cartilage loss in the femorotibial compartments with large subchondral cysts, especially at the tibial plateau

7.6 Concluding Remarks

Knee abnormalities include meniscal, ligamentous, tendinous, bone, and chondral disorders. MRI is highly accurate and is the imaging method of choice to assess internal derangement of the knee. Several new information regarding anatomy and pathology of the menisci, tendons, and ligaments were published in the last years. Recognition of knee anatomy, normal variants, and imaging patterns of main disorders is pivotal for an accurate diagnosis.

Take Home Messages

- MR imaging criteria for a meniscal tear are meniscal morphologic distortion (in absence of prior surgery) or intrameniscal high signal intensity extending to an articular surface, seen on two or more consecutive slices.
- Direct MR signs of an ACL tear are focal ligamentous discontinuity, diffuse or focal signal intensity abnormality, and abnormal orientation of the ACL.

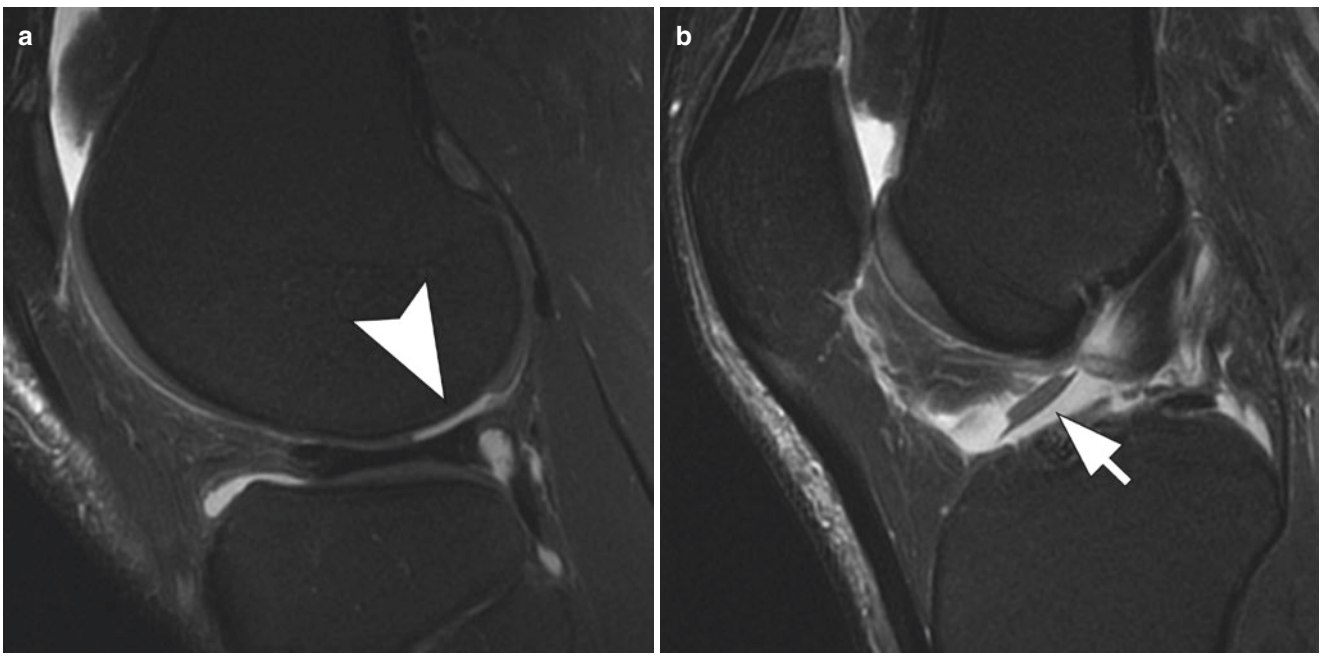

Fig. 7.34 Intraarticular loose body. Sagittal PD-weighted images with fat suppression. (**a**) A deep chondral lesion with sharp margins at the lateral femoral condyle (arrowhead), indicating an acute chondral detachment. (**b**) The chondral fragment is dislocated to the anterior aspect of the intercondylar notch (arrow)

- Main structures involved in posterolateral corner stability are lateral collateral ligament, biceps femoris tendon, popliteus tendon, and popliteofibullar ligament.
- Chondral lesions are characterized on MRI by thickness and morphological abnormalities of hyaline cartilage as well as intrasubstance increased signal on fluid-sensitive sequences.

References

1. Scott WN, Diduch DR, Long WJ. Insall & Scott surgery of the knee. 6th ed. Philadelphia, PA: Elsevier; 2018. 2360 p
2. Resnick D. Diagnosis of bone and joint disorders. 4th ed. Philadelphia, PA: W.B. Saunders Company; 2002.
3. Marcheix PS, Marcheix B, Siegler J, Bouillet P, Chaynes P, Valleix D, et al. The anterior intermeniscal ligament of the knee: an anatomic and MR study. Surg Radiol Anat. 2009;31(5):331–4.
4. Cho JM, Suh JS, Na JB, Cho JH, Kim Y, Yoo WK, et al. Variations in meniscofemoral ligaments at anatomical study and MR imaging. Skelet Radiol. 1999;28(4):189–95.
5. De Smet AA, Asinger DA, Johnson RL. Abnormal superior popliteomeniscal fascicle and posterior pericapsular edema: indirect MR imaging signs of a lateral meniscal tear. Am J Roentgenol. 2001;176(1):63–6.
6. Sanders TG, Linares RC, Lawhorn KW, Tirman PF, Houser C. Oblique meniscomeniscal ligament: another potential pitfall for a meniscal tear--anatomic description and appearance at MR imaging in three cases. Radiology. 1999;213(1):213–6.
7. Nguyen JC, De Smet AA, Graf BK, Rosas HG. MR imaging-based diagnosis and classification of meniscal tears. Radiographics. 2014;34(4):981–99.
8. Monllau JC, León A, Cugat R, Ballester J. Ring-shaped lateral meniscus. Arthroscopy. 1998;14(5):502–4.
9. Yaniv M, Blumberg N. The discoid meniscus. J Child Orthop. 2007;1(2):89–96.
10. Chew FS. Medial meniscal flounce: demonstration on MR imaging of the knee. Am J Roentgenol. 1990;155(1):199.
11. Schnarkowski P, Tirman PF, Fuchigami KD, Crues JV, Butler MG, Genant HK. Meniscal ossicle: radiographic and MR imaging findings. Radiology. 1995;196(1):47–50.
12. De Smet AA, Graf BK. Meniscal tears missed on MR imaging: relationship to meniscal tear patterns and anterior cruciate ligament tears. Am J Roentgenol. 1994;162(4):905–11.
13. Crues JV, Mink J, Levy TL, Lotysch M, Stoller DW. Meniscal tears of the knee: accuracy of MR imaging. Radiology. 1987;164(2):445–8.
14. De Smet AA, Norris MA, Yandow DR, Quintana FA, Graf BK, Keene JS. MR diagnosis of meniscal tears of the knee: importance of high signal in the meniscus that extends to the surface. Am J Roentgenol. 1993;161(1):101–7.
15. De Smet AA, Tuite MJ. Use of the "two-slice-touch" rule for the MRI diagnosis of meniscal tears. Am J Roentgenol. 2006;187(4):911–4.
16. Chahla J, Dean CS, Moatshe G, Mitchell JJ, Cram TR, Yacuzzi C, et al. Meniscal ramp lesions: anatomy, incidence, diagnosis, and treatment. Orthop J Sports Med. 2016;4(7):2325967116657815.
17. Hatayama K, Terauchi M, Saito K, Aoki J, Nonaka S, Higuchi H. Magnetic resonance imaging diagnosis of medial meniscal ramp lesions in patients with anterior cruciate ligament injuries. Arthroscopy. 2018;34(5):1631–7.
18. Balazs GC, Greditzer HG, Wang D, Marom N, Potter HG, Marx RG, et al. Ramp lesions of the medial meniscus in patients undergoing primary and revision ACL reconstruction: prevalence and risk factors. Orthop J Sports Med. 2019;7(5):2325967119843509.
19. Nguyen JC, Bram JT, Lawrence JTR, Hong S, Leska TM, Ganley TJ, et al. MRI criteria for ramp lesions of the knee in children with anterior cruciate ligament tears. Am J Roentgenol 2020.
20. Savoye PY, Ravey JN, Dubois C, Barbier LP, Courvoisier A, Saragaglia D, et al. Magnetic resonance diagnosis of posterior horn tears of the lateral meniscus using a thin axial plane: the zip sign--a preliminary study. Eur Radiol. 2011;21(1):151–9.
21. de Abreu MR, Chung CB, Trudell D, Resnick D. Meniscofemoral ligaments: patterns of tears and pseudotears of the menisci using cadaveric and clinical material. Skelet Radiol. 2007;36(8):729–35.
22. Saad SS, Gorbachova T, Meniscal Tears SM. Scanned, scoped and sculpted. Radiographics. 2015;35(4):1138–9.
23. Magee TH, Hinson GW. MRI of meniscal bucket-handle tears. Skelet Radiol. 1998;27(9):495–9.
24. Dorsay TA, Helms CA. Bucket-handle meniscal tears of the knee: sensitivity and specificity of MRI signs. Skelet Radiol. 2003;32(5):266–72.
25. Hodler J, Haghighi P, Trudell D, Resnick D. The cruciate ligaments of the knee: correlation between MR appearance and gross and histologic findings in cadaveric specimens. Am J Roentgenol. 1992;159(2):357–60.
26. Fitzgerald SW, Remer EM, Friedman H, Rogers LF, Hendrix RW, Schafer MF. MR evaluation of the anterior cruciate ligament: value of supplementing sagittal images with coronal and axial images. Am J Roentgenol. 1993;160(6):1233–7.
27. Lee JK, Yao L, Phelps CT, Wirth CR, Czajka J, Lozman J. Anterior cruciate ligament tears: MR imaging compared with arthroscopy and clinical tests. Radiology. 1988;166(3):861–4.
28. Robertson PL, Schweitzer ME, Bartolozzi AR, Ugoni A. Anterior cruciate ligament tears: evaluation of multiple signs with MR imaging. Radiology. 1994;193(3):829–34.
29. Gentili A, Seeger LL, Yao L, Do HM. Anterior cruciate ligament tear: indirect signs at MR imaging. Radiology. 1994;193(3):835–40.
30. Naraghi A, White LM. MR imaging of cruciate ligaments. Magn Reson Imaging Clin N Am. 2014;22(4):557–80.
31. Kijowski R, Sanogo ML, Lee KS, Muñoz Del Río A, McGuine TA, Baer GS, et al. Short-term clinical importance of osseous injuries diagnosed at MR imaging in patients with anterior cruciate ligament tear. Radiology. 2012;264(2):531–41.
32. Vahey TN, Hunt JE, Shelbourne KD. Anterior translocation of the tibia at MR imaging: a secondary sign of anterior cruciate ligament tear. Radiology. 1993;187(3):817–9.
33. Nakase J, Toratani T, Kosaka M, Ohashi Y, Tsuchiya H. Roles of ACL remnants in knee stability. Knee Surg Sports Traumatol Arthrosc. 2013;21(9):2101–6.
34. Tjoumakaris FP, Donegan DJ, Sekiya JK. Partial tears of the anterior cruciate ligament: diagnosis and treatment. Am J Orthop (Belle Mead NJ). 2011;40(2):92–7.
35. Van Dyck P, De Smet E, Veryser J, Lambrecht V, Gielen JL, Vanhoenacker FM, et al. Partial tear of the anterior cruciate ligament of the knee: injury patterns on MR imaging. Knee Surg Sports Traumatol Arthrosc. 2012;20(2):256–61.
36. Busch MT, Fernandez MD, Aarons C. Partial tears of the anterior cruciate ligament in children and adolescents. Clin Sports Med. 2011;30(4):743–50.
37. Sonin AH, Fitzgerald SW, Hoff FL, Friedman H, Bresler ME. MR imaging of the posterior cruciate ligament: normal, abnormal, and associated injury patterns. Radiographics. 1995;15(3):551–61.
38. Patten RM, Richardson ML, Zink-Brody G, Rolfe BA. Complete vs partial-thickness tears of the posterior cruciate ligament: MR findings. J Comput Assist Tomogr. 1994;18(5):793–9.
39. McMonagle JS, Helms CA, Garrett WE, Vinson EN. Tramtrack appearance of the posterior cruciate ligament (PCL):

correlations with mucoid degeneration, ligamentous stability, and differentiation from PCL tears. Am J Roentgenol. 2013;201(2):394–9.
40. Mariani PP, Margheritini F, Christel P, Bellelli A. Evaluation of posterior cruciate ligament healing: a study using magnetic resonance imaging and stress radiography. Arthroscopy. 2005;21(11):1354–61.
41. Shelbourne KD, Jennings RW, Vahey TN. Magnetic resonance imaging of posterior cruciate ligament injuries: assessment of healing. Am J Knee Surg. 1999;12(4):209–13.
42. Jung YB, Jung HJ, Yang JJ, Yang DL, Lee YS, Song IS, et al. Characterization of spontaneous healing of chronic posterior cruciate ligament injury: Analysis of instability and magnetic resonance imaging. J Magn Reson Imaging. 2008;27(6):1336–40.
43. Warren LF, Marshall JL. The supporting structures and layers on the medial side of the knee: an anatomical analysis. J Bone Joint Surg Am. 1979;61(1):56–62.
44. De Maeseneer M, Van Roy F, Lenchik L, Barbaix E, De Ridder F, Osteaux M. Three layers of the medial capsular and supporting structures of the knee: MR imaging-anatomic correlation. Radiographics. 2000;20 Spec No:S83–9.
45. Wen DY, Propeck T, Kane SM, Godbee MT, Rall KL. MRI description of knee medial collateral ligament abnormalities in the absence of trauma: edema related to osteoarthritis and medial meniscal tears. Magn Reson Imaging. 2007;25(2):209–14.
46. De Maeseneer M, Shahabpour M, Van Roy F, Goossens A, De Ridder F, Clarijs J, et al. MR imaging of the medial collateral ligament bursa: findings in patients and anatomic data derived from cadavers. Am J Roentgenol. 2001;177(4):911–7.
47. Liu F, Yue B, Gadikota HR, Kozanek M, Liu W, Gill TJ, et al. Morphology of the medial collateral ligament of the knee. J Orthop Surg Res. 2010;5:69.
48. Saigo T, Tajima G, Kikuchi S, Yan J, Maruyama M, Sugawara A, et al. Morphology of the insertions of the superficial medial collateral ligament and posterior oblique ligament using 3-dimensional computed tomography: a cadaveric study. Arthroscopy. 2017;33(2):400–7.
49. LaPrade RF, Engebretsen AH, Ly TV, Johansen S, Wentorf FA, Engebretsen L. The anatomy of the medial part of the knee. J Bone Joint Surg Am. 2007;89(9):2000–10.
50. Schweitzer ME, Tran D, Deely DM, Hume EL. Medial collateral ligament injuries: evaluation of multiple signs, prevalence and location of associated bone bruises, and assessment with MR imaging. Radiology. 1995;194(3):825–9.
51. Keyhani S, Mardani-Kivi M. Anatomical repair of Stener-like Lesion of medial collateral ligament: a case series and technical note. Arch Bone Jt Surg. 2017;5(4):255–8.
52. Boutin RD, Fritz RC, Walker REA, Pathria MN, Marder RA, Yao L. Tears in the distal superficial medial collateral ligament: the wave sign and other associated MRI findings. Skelet Radiol. 2020;49(5):747–56.
53. Watanabe Y, Moriya H, Takahashi K, Yamagata M, Sonoda M, Shimada Y, et al. Functional anatomy of the posterolateral structures of the knee. Arthroscopy. 1993;9(1):57–62.
54. LaPrade RF, Terry GC. Injuries to the posterolateral aspect of the knee. Association of anatomic injury patterns with clinical instability. Am J Sports Med. 1997;25(4):433–8.
55. Sanchez AR, Sugalski MT, LaPrade RF. Anatomy and biomechanics of the lateral side of the knee. Sports Med Arthrosc Rev. 2006;14(1):2–11.
56. Rosas HG. Unraveling the posterolateral corner of the knee. Radiographics. 2016;36(6):1776–91.
57. Geiger D, Chang EY, Pathria MN, Chung CB. Posterolateral and posteromedial corner injuries of the knee. Magn Reson Imaging Clin N Am. 2014;22(4):581–99.
58. Moorman CT, LaPrade RF. Anatomy and biomechanics of the posterolateral corner of the knee. J Knee Surg. 2005;18(2):137–45.
59. LaPrade RF, Gilbert TJ, Bollom TS, Wentorf F, Chaljub G. The magnetic resonance imaging appearance of individual structures of the posterolateral knee. A prospective study of normal knees and knees with surgically verified grade III injuries. Am J Sports Med. 2000;28(2):191–9.
60. Terry GC, LaPrade RF. The posterolateral aspect of the knee. Anatomy and surgical approach. Am J Sports Med. 1996;24(6):732–9.
61. Recondo JA, Salvador E, Villanúa JA, Barrera MC, Gervás C, Alústiza JM. Lateral stabilizing structures of the knee: functional anatomy and injuries assessed with MR imaging. Radiographics. 2000;20 Spec No:S91–S102.
62. Lee J, Papakonstantinou O, Brookenthal KR, Trudell D, Resnick DL. Arcuate sign of posterolateral knee injuries: anatomic, radiographic, and MR imaging data related to patterns of injury. Skelet Radiol. 2003;32(11):619–27.
63. Maynard MJ, Deng X, Wickiewicz TL, Warren RF. The popliteofibular ligament. Rediscovery of a key element in posterolateral stability. Am J Sports Med. 1996;24(3):311–6.
64. Rajeswaran G, Lee JC, Healy JC. MRI of the popliteofibular ligament: isotropic 3D WE-DESS versus coronal oblique fat-suppressed T2W MRI. Skelet Radiol. 2007;36(12):1141–6.
65. Collins MS, Bond JR, Crush AB, Stuart MJ, King AH, Levy BA. MRI injury patterns in surgically confirmed and reconstructed posterolateral corner knee injuries. Knee Surg Sports Traumatol Arthrosc. 2015;23(10):2943–9.
66. Sims WF, Jacobson KE. The posteromedial corner of the knee: medial-sided injury patterns revisited. Am J Sports Med. 2004;32(2):337–45.
67. Claes S, Vereecke E, Maes M, Victor J, Verdonk P, Bellemans J. Anatomy of the anterolateral ligament of the knee. J Anat. 2013;223(4):321–8.
68. Helito CP, Demange MK, Helito PV, Costa HP, Bonadio MB, Pecora JR, et al. Evaluation of the anterolateral ligament of the knee by means of magnetic resonance examination. Rev Bras Ortop. 2015;50(2):214–9.
69. Helito CP, Helito PV, Costa HP, Bordalo-Rodrigues M, Pecora JR, Camanho GL, et al. MRI evaluation of the anterolateral ligament of the knee: assessment in routine 1.5-T scans. Skelet Radiol. 2014;43(10):1421–7.
70. Caterine S, Litchfield R, Johnson M, Chronik B, Getgood A. A cadaveric study of the anterolateral ligament: re-introducing the lateral capsular ligament. Knee Surg Sports Traumatol Arthrosc. 2015;23(11):3186–95.
71. Claes S, Luyckx T, Vereecke E, Bellemans J. The Segond fracture: a bony injury of the anterolateral ligament of the knee. Arthroscopy. 2014;30(11):1475–82.
72. Helito PVP, Bartholomeeusen S, Claes S, Rodrigues MB, Helito CP. Magnetic resonance imaging evaluation of the anterolateral ligament and the iliotibial band in acute anterior cruciate ligament injuries associated with segond fractures. Arthroscopy. 2020;36(6):1679–86.
73. Flato R, Passanante GJ, Skalski MR, Patel DB, White EA, Matcuk GR. The iliotibial tract: imaging, anatomy, injuries, and other pathology. Skelet Radiol. 2017;46(5):605–22.
74. Mansour R, Yoong P, McKean D, Teh JL. The iliotibial band in acute knee trauma: patterns of injury on MR imaging. Skelet Radiol. 2014;43(10):1369–75.
75. Sonin AH, Fitzgerald SW, Bresler ME, Kirsch MD, Hoff FL, Friedman H. MR imaging appearance of the extensor mechanism of the knee: functional anatomy and injury patterns. Radiographics. 1995;15(2):367–82.
76. Azer NM, Winalski CS, Minas T. MR imaging for surgical planning and postoperative assessment in early osteoarthritis. Radiol Clin N Am. 2004;42(1):43–60.
77. Vande Berg BC, Lecouvet FE, Poilvache P, Jamart J, Materne R, Lengele B, et al. Assessment of knee cartilage in cadavers with

dual-detector spiral CT arthrography and MR imaging. Radiology. 2002;222(2):430–6.
78. Vande Berg BC, Lecouvet FE, Malghem J. Frequency and topography of lesions of the femoro-tibial cartilage at spiral CT arthrography of the knee: a study in patients with normal knee radiographs and without history of trauma. Skelet Radiol. 2002;31(11):643–9.
79. Outerbridge RE. The etiology of chondromalacia patellae. J Bone Joint Surg Br. 1961;43-B:752–7.
80. Brittberg M, Winalski CS. Evaluation of cartilage injuries and repair. J Bone Joint Surg Am. 2003;85-A(Suppl 2):58–69.
81. Carrino JA, Blum J, Parellada JA, Schweitzer ME, Morrison WB. MRI of bone marrow edema-like signal in the pathogenesis of subchondral cysts. Osteoarthr Cartil. 2006;14(10):1081–5.